DYNAMICS OF WEATHER AND CLIMATE VARIABILITY OVER THE ALL-YEAR RAINFALL REGION OF SOUTH AFRICA

Report to the
Water Research Commission

by

CJ Engelbrecht[1,2] & WA Landman[3]

[1]Agricultural Research Council, Institute for Soil, Climate and Water
[2]Department of Geography, Geoinformatics and Meteorology,
University of Pretoria
[3]Council for Scientific and Industrial Research

WRC Report No.2257/1/15
ISBN 978-1-4312-0756-5

January 2016

Obtainable from
Water Research Commission
Private Bag X03
Gezina, 0031

orders@wrc.org.za or download from www.wrc.org.za

DISCLAIMER

This report has been reviewed by the Water Research Commission (WRC) and approved for publication. Approval does not signify that the contents necessarily reflect the views and policies of the WRC nor does mention of trade names or commercial products constitute endorsement or recommendation for use.

© Water Research Commission

Executive Summary

Introduction and Objectives

Climatologically, the Cape south coast is unique in the sense that it lacks the pronounced seasonality observed over the remainder of South Africa. Here, rainfall occurs all-year round, implying that rainfall-producing systems characteristic of both the winter and summer rainfall regions contribute to rainfall over the Cape south coast. However, the relative contributions of different rain-producing weather systems to annual rainfall have not been quantified to date. This region has also not received as much attention as the winter and summer rainfall regions of the country with regards to quantifying and understanding their interannual rainfall variability. This study addresses these issues through objective identification of the prevailing synoptic types of the Cape south coast region, with a subsequent analysis of their interannual variability. The association between synoptic types and streamflow is also investigated.

The specific objectives of the project were:

1. Determine the relative contribution of the various rain-producing synoptic scale weather systems to monthly and seasonal rainfall totals over the all-year rainfall region.
2. Determine the relative contribution of the various rain-producing synoptic scale weather systems to the rainfall peaks observed in the annual rainfall cycle.
3. Determine if there is significant variability in the occurrence of rain producing synoptic scale weather systems during wet and dry seasons.
4. Determine the association between synoptic scale weather systems and streamflow over the all-year rainfall region.

Results and Conclusions

The relative contribution of different rain-producing systems to annual rainfall over the Cape south coast is quantified. Ridging high pressure systems contribute most to the mean annual rainfall (46%), followed by tropical-temperate troughs (28%) and cut-off lows (COLs). COLs, co-occurring with ridging high pressure systems and tropical-temperate troughs, contribute to 16% of the mean annual rainfall. When extreme rainfall is considered, COLs contribute to 29% of all extreme rainfall events along the Cape south coast. Particular configurations of ridging high pressure systems and tropical-temperate troughs that are linked to interannual variability of seasonal rainfall are identified. These systems are primarily ridging high pressure systems, in particular those ridging from far south of the subcontinent, and tropical-temperate troughs occurring during seasons with weaker zonal mid- and upper air winds. COLs are also linked to interannual variability of seasonal rainfall, despite their infrequent occurrence – highlighting the importance of COLs as high impact weather systems. The COL link with rainfall variability is particularly strong during March-April-May (MAM) and even more so for June-July-August (JJA).

Knowledge Dissemination

Engelbrecht CJ, Landman WA and Engelbrecht FA. 2012. The all-year rainfall region of South Africa: satellite rainfall-estimate perspective. 28th Annual Conference of the South African society for Atmospheric Sciences, September 2012, Cape Town

Engelbrecht CJ, Landman WA and Engelbrecht FA. 2013. The relative contribution of synoptic types to rainfall over the Cape south coast region. 29th Annual Conference of the South African society for Atmospheric Sciences, September 2013, Durban

Engelbrecht CJ and Landman WA. 2014. Interannual rainfall variability over the Cape south coast of South Africa linked to cut-off low associated rainfall. 30th Annual Conference of the South African society for Atmospheric Sciences, October 2014, Potchefstroom

Engelbrecht CJ, Landman WA, Engelbrecht FA and Malherbe J. 2015. A synoptic decomposition of rainfall over the Cape south coast of South Africa. Climate Dynamics 44:2589-2607. DOI 10.1007/s00382-014-2230-5

Engelbrecht CJ and Landman WA. 2015. Interannual variability of seasonal rainfall over the Cape south coast of South Africa and synoptic type association. Climate Dynamics. DOI 10.1007/s00382-015-2836-2

Capacity Building

Christien Engelbrecht, PhD(Meteorology), University of Pretoria, 2016.
The technique of Self-Organizing Maps (SOMs) was mastered during this project and have continued to transfer this knowledge to other meteorologists and climatologists.

Acknowledgements

Thank you very much to the Water Research Commission for funding this project and PhD study.

The contribution by the reference group members is also acknowledged. They are:
Mr W Nomquphu (Chair: WRC)
Mr A Beraki (SAWS)
Dr L Dyson (UP)
Mrs S Landman (SAWS)
Dr C Lennard (UCT)
Dr C Moseki (WRC when this project commenced)
Dr J Malherbe (ARC)
Dr T Ndarana (CSIR)
Prof G Pegram (Pegram & Associates)
Prof C Reason (UCT)
Mr D van der Mescht

List of abbreviations

AOH	Atlantic Ocean High
ARC	Agricultural Research Council
COL	Cut-Off Low
CRU	Climatic Research Unit
DEM	Digital Elevation Model
DJF	December-January-February
ENSO	El Niño Southern Oscillation
FEWS	Famine Early Warning System
JAS	July-August-September
JJA	June-July-August
MAM	March-April-May
NCEP	National Centers for Environmental Prediction
OND	October-November-December
RE	Ridging high pressure system situated East/southeast of the subcontinent
RSW	Ridging high pressure system from the SouthWest of the subcontinent
SAM	Southern Annular Mode
SAWS	South African Weather Service
SLP	Sea-level pressure
SOM	Self-Organizing Map
SON	September-October-November
SRTM	Shuttle Radar Topography Mission
TSE	Trough SouthEast of the subcontinent
TSW	Trough SouthWest of the subcontinent
TTT	Tropical-Temperate Trough
WSF	Weak Synoptic Flow

Table of contents

Chapter 1: Introduction

1.1 The all-year rainfall region

The all-year rainfall region of South Africa (Fig. 1.1) is found as a narrow strip along the Cape south coast (Taljaard, 1996; Weldon and Reason, 2014) between approximately 21°E and 27°E and mostly on the seaward side of the Cape Folded mountain range (Engelbrecht et al., 2015). The all-year nature of rainfall of this region is in strong contrast to the seasonality that characterizes rainfall over most of South Africa: the country is largely a summer rainfall region (e.g. Fauchereau et al., 2009), with winter rainfall occurring over the southwestern Cape area (e.g. Philippon et al., 2011). The all-year rainfall region of the Cape south coast may to some extent be thought of as forming a boundary region between the winter and summer rainfall regions and consequently recieves rainfall from weather systems both responsible for rainfall over the summer and winter rainfall regions, like tropical-temperate troughs and cold fronts respectively. However, the all-year rainfall region also receives rainfall from weather systems such as ridging high pressure systems (Jury and Levey, 1993; Favre et al., 2013; Weldon and Reason, 2014). Ridging high pressure systems is not directly responsible for rainfall over the other rainfall regions of the country, in particular the winter rainfall region. Over the summer rainfall region ridging high pressure systems play an important role in moisture advection and aid in strengthening of the surface trough (Taljaard, 1996) that can in turn act as a trigger mechanism for convective rainfall. Another important rain-bearing weather system is the COL. COLs are responsible for rainfall countrywide but explain a higher proportion of rainfall over the Cape south coast region of South Africa compared to the winter and summer rainfall regions (Favre et al., 2013). The impact COLs can have on rainfall is also illustrated by the occurrence of winter rainfall over the summer rainfall region that is usually COL-induced (Taljaard, 1996). The weather systems mentioned above (tropical-temperate troughs, cold fronts, ridging high pressure systems and COLs) are all well-defined synoptic scale weather systems – complex interactions and linkages between these systems can occur and contribute to the unique rainfall characteristics of the all-year rainfall region. Superimposed on the synoptic circulation there are also meso-scale circulation systems, which result from interactions of the larger scale flow with mountainous topography inland of the coastal areas and the moisture laden air above the Agulhas current flowing along the Cape south coast of South Africa (e.g. Rouault et al., 2002; Singleton and Reason, 2006). Regional climate gradients over the all-year rainfall region can be attributed to the interaction of the larger-scale flow with topography and the oceanic influences.

South Africa is considered an arid country and only 8% of the land area produces 50% of the surface run-off (Nel et al., 2013). There are 21 water source areas over South Africa and four of these water source areas, namely the Outeniqua, Kougaberg, Langeberg and Tsitsikamma are located within the all-year rainfall region. Despite the importance of precipitation contributing to run-off and subsequently inflow into reservoirs, a knowledge gap exists with regard to the contribution to rainfall by synoptic-scale weather systems over the all-year rainfall region as well as the behaviour of synoptic-scale weather systems associated with interannual rainfall variability. Droughts and floods occur from time to time over the all-year rainfall region. Both droughts and floods can have a severe negative impact on the region, for example the drought that occurred between 2009 and 2011 as well as the November 2007 and October 2012 flood events that caused damage to infrastructure. In recent studies the contribution of COLs (Favre et al., 2013) and tropical-temperate troughs (Hart et al., 2013) to rainfall over South Africa have been addressed. With regard to the all-year rainfall region it still needs to be determined what the contribution of ridging high pressure systems and cold fronts are. An increase in water demand is experienced over the Cape south coast region due to urbanisation (e.g. Holloway et al., 2012). On top of the urbanisation related increase in water demand, a warming climate is also projected to contribute to an increase in water demand (Christensen et al., 2007). Within the context of the all-year rainfall region, there is thus a need to extend our current understanding of synoptic circulation and the associated rainfall to include all seasons and all synoptic types.

1.2 Drainage regions over the all-year rainfall region

The geographical location of the all-year rainfall region of South Africa relative to the primary catchments over the country is shown in Figure 1.1.

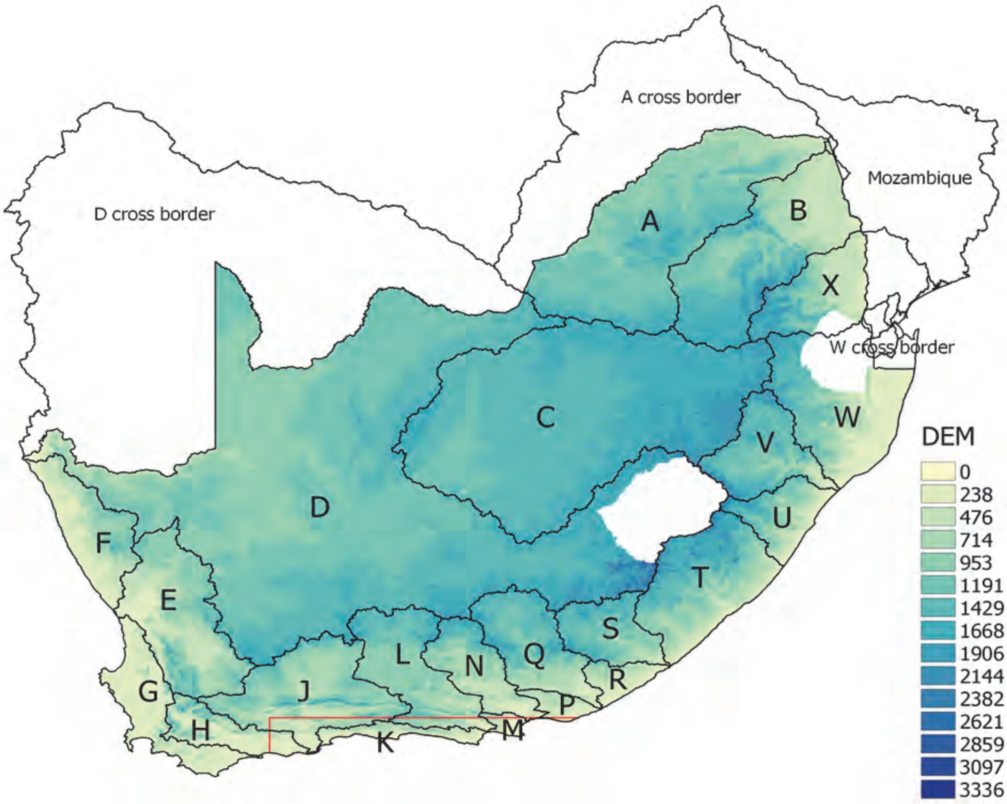

Figure 1.1 The primary catchments over Southern Africa are delineated by the solid black lines. The all-year rainfall region is delineated by the red solid lines. The primary catchment identification indicator is indicated in black. The topography over the country as represented by the SRTM DEM is shown in yellow, green and blue shades.

Of the primary catchments, only the K-drainage region is located completely within the all-year rainfall region. Small portions of drainage regions H, J, L, M, N and P are also located within the all-year rainfall region (Fig. 1.1). The larger part of drainage region H falls within the winter rainfall region, while drainage regions J, L, M, N and P are largely located within the summer rainfall region of South Africa. The geographical location of water reservoirs over the all-year rainfall region is shown in Figure 1.2.

Figure 1.2 Location of water reservoirs over the all-year rainfall region.

The Hartebeeskuil, Kouga, Groendal, Ernest Robertson, Garden Route and Krom water reservoirs are located in water source areas and all of them with the exception of Kouga and Groendal are located within drainage region K. Adequate rainfall in particular over drainage region K is thus necessary to sustain agricultural practices over most of the all-year rainfall region as well as for water supply to the towns and cities found along the coast. The association between synoptic scale weather systems and streamflow is therefore investigated.

Chapter 2: Attributes of rainfall over the all-year rainfall region of South Africa

2.1 Spatial extent of the all-year rainfall region

Two independently constructed gridded rainfall datasets, the Famine Early Warning System (FEWS) and the Climatic Research Unit (CRU) version TS3.1, were utilized for revisiting the delineation of the all-year rainfall region. Gridded data were used for this purpose rather than station data, due to the uneven distribution in space of stations with records of sufficient length and quality. The FEWS data are a merged satellite-gauge gridded daily rainfall dataset with a resolution of 0.1˚ longitude by 0.1˚ latitude, with records commencing in January 1983 (Sylla et al., 2013). The CRU TS3.1 monthly gridded rainfall dataset has a resolution of 0.5˚ longitude by 0.5˚ latitude, is based solely on station data and is available for the period 1901 to 2009 (Harris et al., 2014). The all-year rainfall region may be defined using the following criteria as guidelines:

- The ratio of the rainfall amount for the month of minimum rainfall to rainfall of the month of maximum rainfall is relatively high (40% or more) compared to regions of strong seasonality.
- Each month of the year needs to be associated with at least 5% of the annual rainfall. This 5% threshold is based on graphs produced by Taljaard (1996), where the monthly contribution to the annual rainfall for various rainfall regions as identified by van Rooy (1972) is presented.
- The average monthly fluctuation of rainfall relative to the average monthly rainfall over the all-year rainfall region should be small compared to that of the winter and summer rainfall regions.

It may be noted that prior to using the gridded datasets for the purpose of identifying the spatial extent of the all-year rainfall region, it was first established that these rainfall sets sufficiently describe the annual rainfall cycle over South Africa. This was achieved through a comparison of the monthly rainfall climatologies of the gridded datasets against those of weather stations. Despite the general underestimation of rainfall totals over Africa in FEWS data, in particular over regions of orography (Sylla et al., 2013), both datasets have been found to give representations of the annual rainfall cycle of all-year rainfall consistent with the raw weather station data.

Application of the criteria describing all-year rainfall attributes on CRU TS3.1 and FEWS mean monthly rainfall data, yields remarkably similar spatial patterns (Fig. 2.1) – across the 3 different metrics, and across the 2 data sets. Qualitatively, the metrics indicate that the spatial extent of the area receiving rainfall all-year round along the Cape south coast is found within the collective boundaries described in other studies (e.g. Taljaard, 1996;

Landman et al., 2001a; Rouault and Richard, 2003; Weldon and Reason, 2014). Along the coast, the all-year rainfall region is found approximately between 21° E and 27° E, while its northern extent is mostly restricted by the Cape Folded mountain range. The extent of the all-year rainfall region is well illustrated by the metric of the number of months of the year that receive 5% or more of the annual rainfall. In both CRU (Fig. 2.1c) and FEWS (Fig. 2.1d), 11-12 months of the year satisfies the criteria over the mentioned area. The twelve weather stations in Figure 2.2 are located in this region – and all receive 5% or more of the annual rainfall total during each month of the year. This region is regarded to define the Cape south coast (or all-year rainfall) region. The data from these twelve weather stations as seen on Figure 2.2 are used for the analysis concerning rainfall attributes in this study. From the western part of the all-year rainfall region along the Cape south coast, a relatively narrow region that exhibits pseudo all-year rainfall characteristics extends northwards, to the east of the western escarpment (see the arrows in Figs. 2.1c and 2.1d). As the main focus of this study is on the Cape south coast, this secondary all-year rainfall region is not considered for analyses. It may finally be noted that there is a small area along the north coast of KwaZulu-Natal that also exhibits all-year rainfall attributes, according to the metrics presented in Figure 2.1. The circulation dynamics of this region are likely to be very different to that of the Cape south coast, and its investigation falls beyond the scope of the current study.

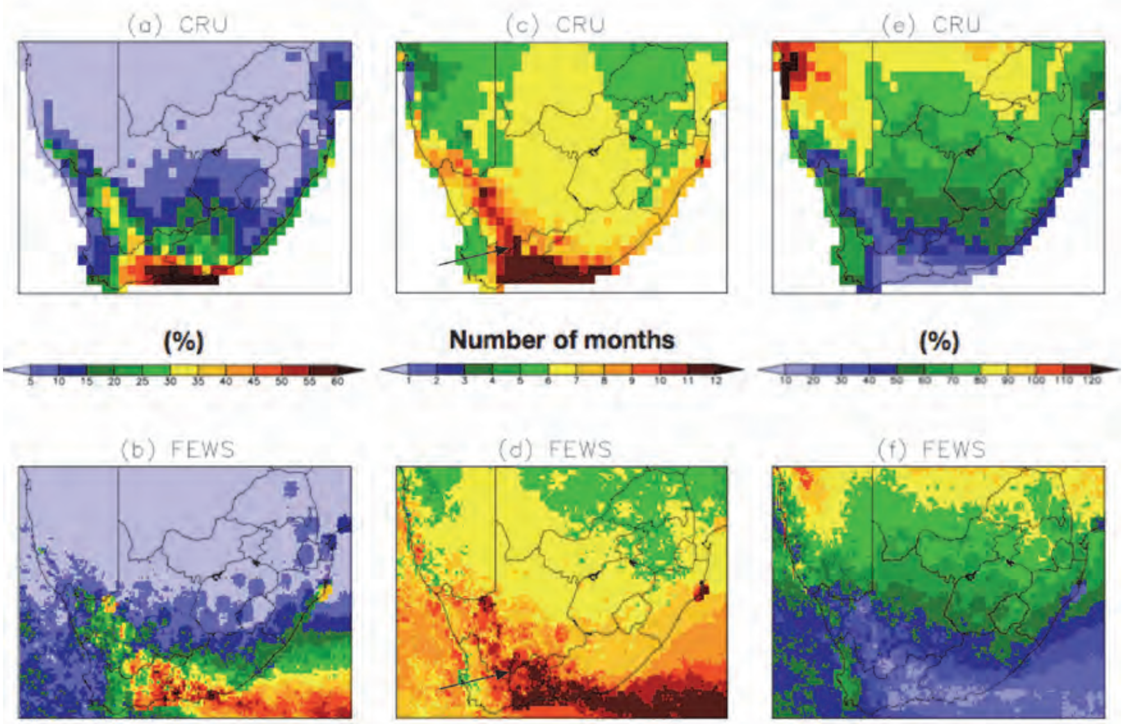

Figure 2.1 Delineation of rainfall regions in South Africa according to the ratio of the month of minimum rainfall to the month of maximum rainfall (a, b), the number of months for which the mean monthly rainfall total contributes 5% or more to the mean annual rainfall total (c, d), and the average fluctuation of monthly rainfall from the monthly mean rainfall expressed as a percentage (e, f), calculated from CRU (a, c, e) and FEWS (b, d, f) data for the period 1983-2009.

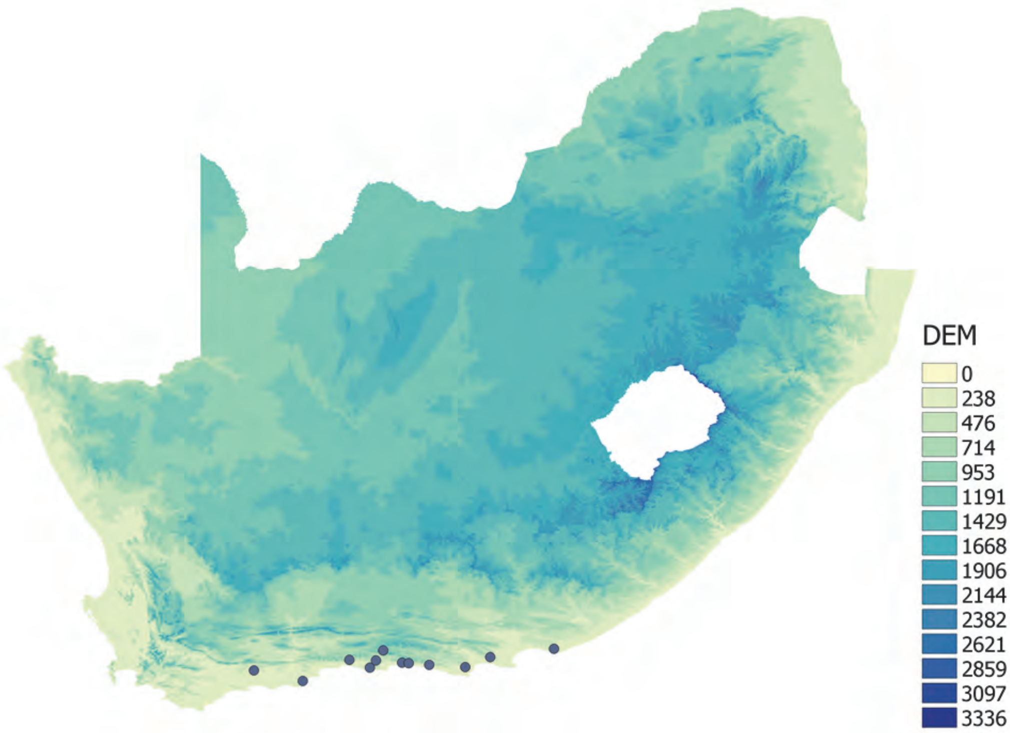

Figure 2.2 Geographical location of the twelve rainfall stations used for rainfall analysis in this study. The circles represent the location of each of the twelve rainfall stations and the shading the topography in meters.

2.2 Annual rainfall cycle

Daily rainfall data for the 33-year period from 1979 to 2011 from twelve weather stations of the South African Weather Service (SAWS) over the Cape south coast were considered in this study (Fig. 2.2). These twelve stations were chosen based on their availability (defined here as the presence of data on more than 90% of the days in a specific month) and quality. Extreme and missing value tests were employed as data quality measures. Values that did not comply with these tests were replaced by estimated values derived from neighbouring stations.

The annual rainfall cycle over the all-year rainfall region of South Africa exhibits small peaks during the transitional seasons (Taljaard, 1996). The all-year rainfall region exhibits three rainfall peaks (Fig. 2.3). These peaks occur during March-April, August and October, with the October peak of 80 mm being the highest (monthly totals averaged over the period 1979-2011 are shown). A rainfall hiatus occurs in September. An objective of the study is to explain the existence of the three rainfall peaks of the all-year rainfall region, from a synoptic type perspective.

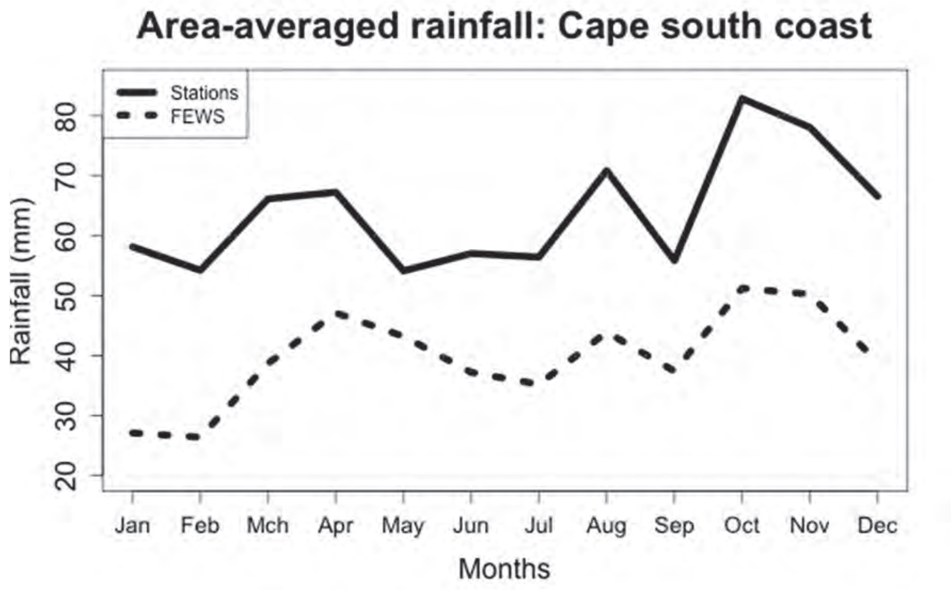

Figure 2.3 Area-averaged annual rainfall cycle for the period 1979-2011 over the all-year rainfall region as described by weather station data (solid line) and FEWS rainfall (dotted line).

2.3 Summary

Regarding the delineation of the all-year rainfall region, the application of the all-year rainfall criteria on CRU and FEWS rainfall data produced in general similar results and is useful to describe the spatial extent of the region. Application of the criteria to the weather station data produced consistent results. Similarly, the annual rainfall cycle described by the weather station data for the all-year rainfall region is qualitatively captured by the FEWS rainfall estimates (Fig. 2.3) and CRU data (not shown). That is, despite the monthly rainfall totals being underestimated by FEWS, the annual rainfall cycle with respect to the peaks and September hiatus is captured. All subsequent rainfall analyses presented in this study are based on the weather station data.

Chapter 3: Synoptic decomposition of rainfall over the all-year rainfall region

3.1 Weather pattern identification

Weather patterns that influence the Cape south coast region of South Africa were objectively identified by application of the self-organizing map (SOM) technique (Kohonen, 2001). The technique is based on an unsupervised nonlinear clustering algorithm that organizes the input data into a user-specified number of nodes that span the continuum of types in the input data. The technique is well suited for weather pattern identification where the daily transitions between weather patterns are important (Hewitson and Crane, 2002). SOMs are increasingly being employed in climate studies focusing on the southern African region (e.g. Hewitson and Crane, 2002; Tennant and Hewitson, 2002; Tozuka et al., 2014; Van Schalkwyk and Dyson, 2013). NCEP reanalysis daily averaged SLP data for the period 1979-2011 was used to develop a SOM relevant to the Cape south coast region. Atmospheric circulation, here the SLP circulation, is driven by the SLP gradients and do not depend on the actual magnitudes of the SLP (Schuenemann et al., 2009). To obtain the required daily gradient fields, the daily domain average of SLP was subtracted from the SLP at each grid point. The SOM was constructed for the region 45° S to 32.5° S and 10° E to 40° E. The selected region allows for capturing the progression of high pressure systems and troughs, advancing from west to east, to the south of the Cape south coast. The northern boundary of the SOM region was purposefully selected to extend to only 32.5° S. If this boundary is chosen further to the north, to include most of the interior of South Africa, the synoptic types identified by the SOM are dominated by the prevailing wintertime high pressure systems over the interior. Furthermore, SLP is used as a variable to develop the SOM, as the circulation over the oceans bordering the subcontinent is crucial in inducing rainfall over the Cape south coast. It may be noted that tropical-temperate trough linkages are captured with the SOM configuration as described, even though the northern boundary of the SOM region is limited to the extreme southern parts of the interior. The typical SLP patterns associated with COLs (e.g. Taljaard, 1985; Tennant and van Heerden, 1994) are also captured. For the purpose of this study, it is appropriate to apply a relatively large SOM to avoid over generalizing the richness of weather patterns that occur over the region into a too small number of nodes (synoptic types). SOMs that classify daily SLP circulation into 12, 20 and 35 synoptic types, respectively, have been considered. It was found that the 12 and 20 node SOMs do not capture the various stages of sea-level anticyclones, ridges and troughs adequately. Of particular importance, is that the known variations in the position and amplitude of SLP ridges and troughs that are representative of weather patterns ranging from weak synoptic flow to tropical-temperate troughs and COLs, are well represented in the SOM. Capturing the variations in ridging anticyclones is important as the rainfall produced by these systems is influenced by the nature of the onshore flow onto the coastal mountains (e.g. Taljaard, 1985; Weldon and Reason, 2014). Topographically induced rainfall occurs on the seaward side of the west-east orientated Cape Folded mountain range along the Cape south coast (Philippon et al., 2011), where strong topographic gradients are found (Singleton and Reason, 2006). Figure 3.1 shows a map of the topography as represented by the Shuttle Radar Topography Mission (SRTM) Digital Elevation Model (DEM) data (Weepener et al., 2012). Some peaks of the Cape Folded mountain range are of comparable elevation to the mountains found over the interior plateau located further northwards (Fig. 3.1).

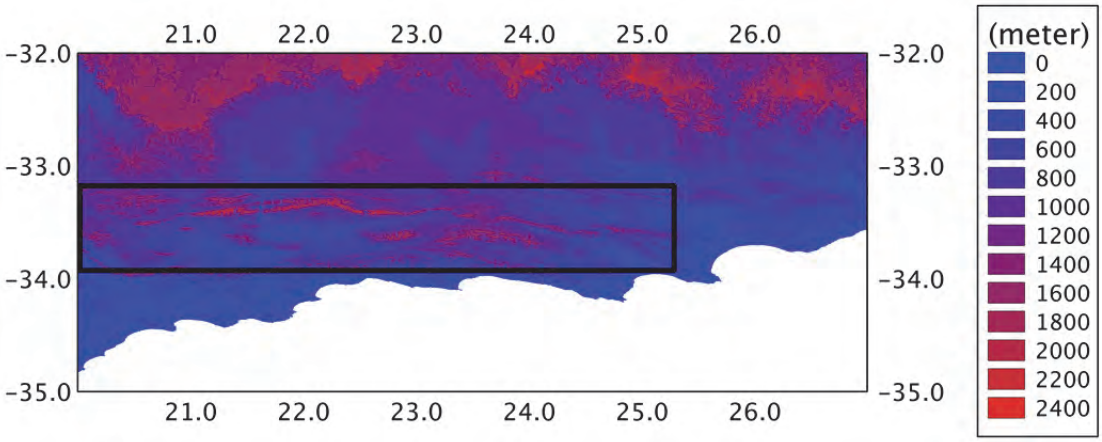

Figure 3.1 Topography of the Cape south coast as represented by SRTM DEM data. The Cape Folded mountain range is indicated by the black rectangle.

3.2 Identification of cut-off lows

COLs (Figure 3.2) are cold-cored closed cyclones in the middle and upper troposphere. COLs develop in the westerlies, equatorwards of the polar jetstream (Taljaard, 1985; Favre et al., 2012). On the average, only about 11 COLs occur annually over the southern African region (Singleton and Reason, 2007b), implying that these systems would not feature as a stand-alone synoptic type in the 7x5 SOM based on daily circulation fields presented in this paper. Indeed, COLs may occur in conjunction with a number of different low-level circulation patterns – most commonly in association with a strong ridge of high pressure in the low-levels polewards of the upper COL (e.g. Taljaard, 1985; Tennant and van Heerden, 1994; Katzfey and McInnes, 1996; Favre et al., 2012), in combination with tropical-temperate troughs (Hart et al., 2013), and further, as a COL system evolves, in association with the evolving high pressure system (ridging progressively from the southwest to southeast of South Africa). The typical low-level circulation associated with tropical-temperate troughs – a meridional trough that links the Angola low and a mid-latitude wave/cyclone, is illustrated in Tennant (2003) and Hart et al. (2010, 2012). An objective tracking methodology is therefore used in order to study the effects of these important rainfall producing systems on rainfall attributes over the Cape south coast region.

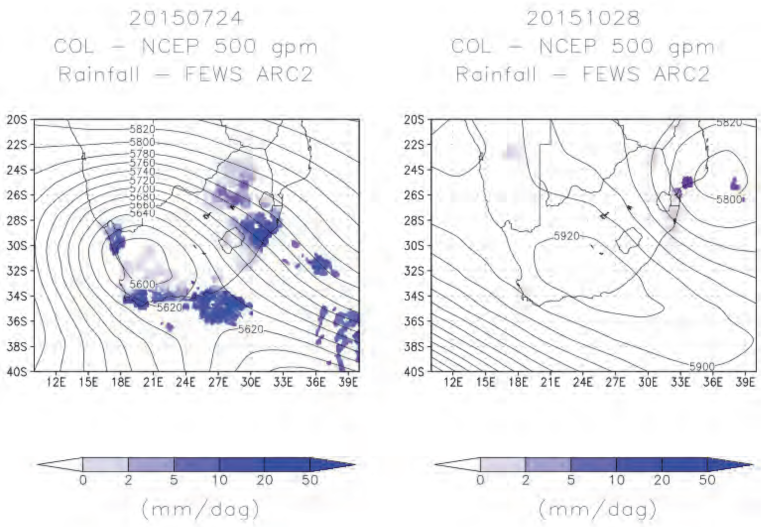

Figure 3.2 COLs as represented in NCEP reanalysis fields of the geopotential height of the 500 hPa pressure level and the associated FEWS ARC2 rainfall estimates for 24 July 2015 (left) and 28 October 2015 (right).

National Center for Environmental Prediction (NCEP) reanalysis data (Kalnay et al., 1996) was utilized for the purpose of identifying and tracking COLs over the period 1979-2011. Over South Africa, COLs exhibit a typical length scale of 1000 km (e.g. Singleton and Reason, 2007b) and are therefore well resolved on the 2.5˚ resolution grid of the NCEP data. In that paper, a COL is defined as a closed-low (a local minimum in the geopotential height at the 500 hPa level) that possesses a cold core, following the criteria used by Favre et al. (2012). The daily-average geopotential height and temperature fields at 500 hPa are utilized for identifying and tracking COLs. All COLs that occurred for at least 24-hours within the domain bounded by 40˚ S – 20˚ S and 10˚ E – 40˚ E are considered in this study. The closed-lows are identified and tracked by applying an objective, automated tracking algorithm. Geopotential minima are identified by comparing the geopotential of each grid point in the domain bounded by 40˚ S – 20˚ S and 10˚ E – 40˚ E, to the geopotential values of the square of eight surrounding grid points on the latitude longitude grid. Closed-low tracks are constructed by identifying the geopotential minima of time step *t+1* nearest to the geopotential minima at time step *t,* provided that this distance is less than 1000 km. This distance implies that closed-lows are assumed to have a mean daily speed that do not exceed 42 km/h (Favre et al., 2012). The tracking procedure is developed in such a manner that any geopotential minimum can only be part of a single track (see Engelbrecht et al., 2013 for details). To identify the COL tracks from the database of closed-low tracks, the approach utilized by Favre et al. (2012) is applied in this study. Each of the closed-low tracks identified through the procedure outlined above is subsequently subjected to tests described in Favre et al. (2012) to ensure that it is of extra-tropical origin, detached from the westerlies and has a cold-core. Figure 3.3 and 3.4 show the geographical distribution (expressed as the number of COL days per grid point) and the annual cycle in the number of COLs for the domain 40˚ S – 20˚ S and 10˚ E – 40˚ E respectively. There are two geographical regions of preferred COL day occurrence, namely in the Mozambique Channel as well as over the Atlantic Ocean extending in over the southwestern part of South Africa (Fig. 3.3). The spatial pattern of the geographical distribution of COL days identified in this study is in good agreement with that of Favre et al. (2013), while the two regions of preferred COL occurrence correspond with the two quadrants representative of the highest frequency distribution of the number of COLs as found by Singleton and Reason (2007b). The COL examples in Figure 3.2 illustrate specific COL events over these two preferred regions of COL occurrence. COLs over the northeastern part of South Africa or the Mozambique Channel are generally not directly responsible for rainfall over the Cape south coast. COL events peak during autumn (Fig. 3.4, March-May) with the least occurrence in November-January (Fig. 3.4), consistent with the findings of Taljaard (1985), Singleton and Reason (2007b) and Favre et al. (2013).

Rainfall associated with cold-cored systems occurs mainly some hundreds of kilometers to the northeast, east and southeast of the centers of these systems (Taljaard, 1995). From the constructed COL dataset for the period 1979-2011, all the COLs that occurred west of 32.5 °E were considered to be potentially responsible for rainfall over the region (e.g Favre et al., 2013). Such COLs associated with rainfall over the study region, at least at a single station, are defined as rainfall producing COLs. Finally, for each day that a COL was identified as a rain-producing weather system over the study area, the circulation of that day was mapped onto the synoptic types identified by the SOM. This enables the identification of the synoptic types that are most frequently associated with COLs that influence the study area.

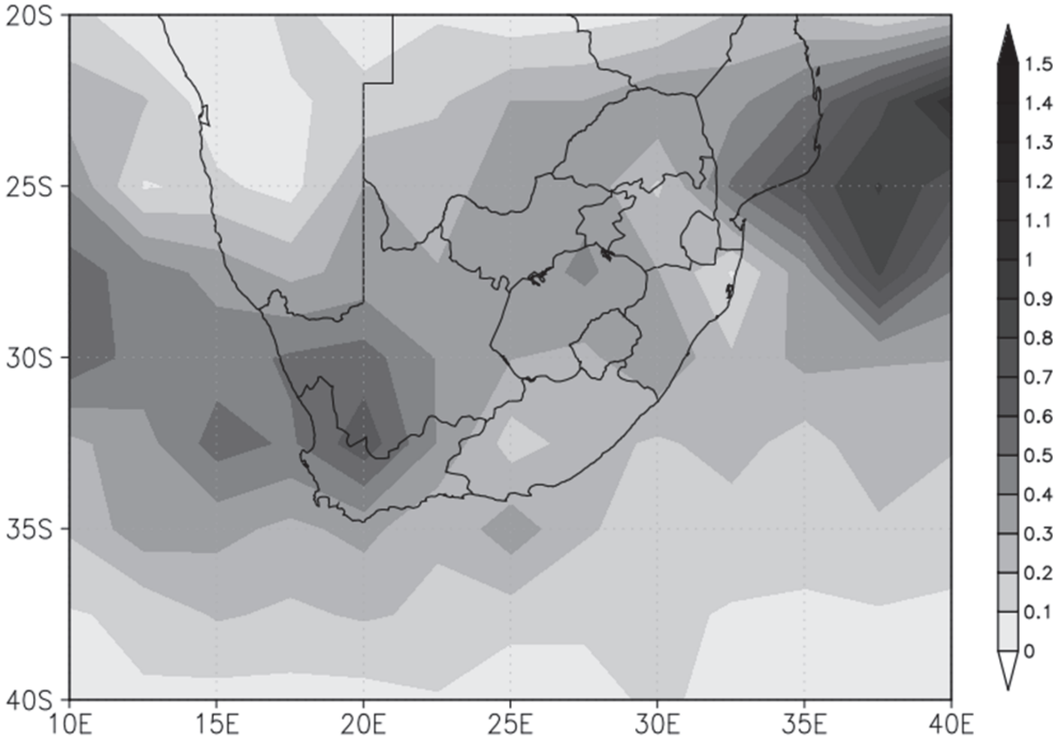

Figure 3.3 Mean annual COL frequency over the domain 40˚ S – 20˚ S and 10˚ E – 40˚ E expressed as the number of COL days per grid point.

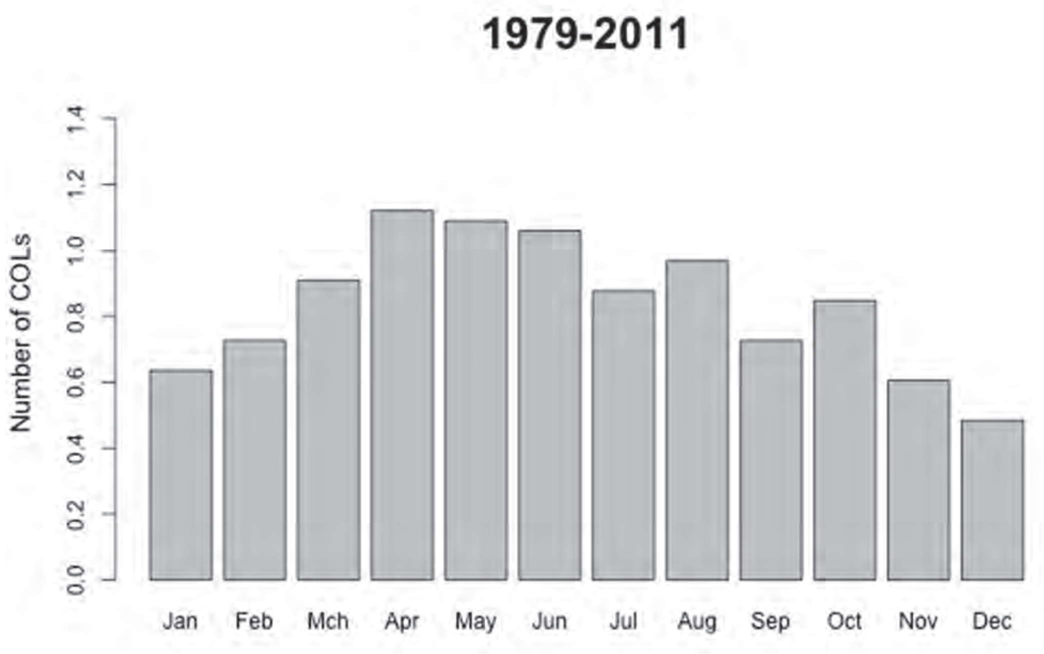

Figure 3.4 Annual cycle of COLs over the domain 40˚ S – 20˚ S and 10˚ E – 40˚ E expressed as the monthly mean number of COL events.

3.3 Synoptic type classification

Figure 3.5 shows the synoptic type classification produced by the SOM algorithm. Each node in the SOM represents a single SLP anomaly pattern representative of a portion of the 12053 daily patterns used to train the SOM. The frequency of occurrence for each of the nodes is indicated at the top right of the relevant node, with the node number shown at the top left (Fig. 3.5).

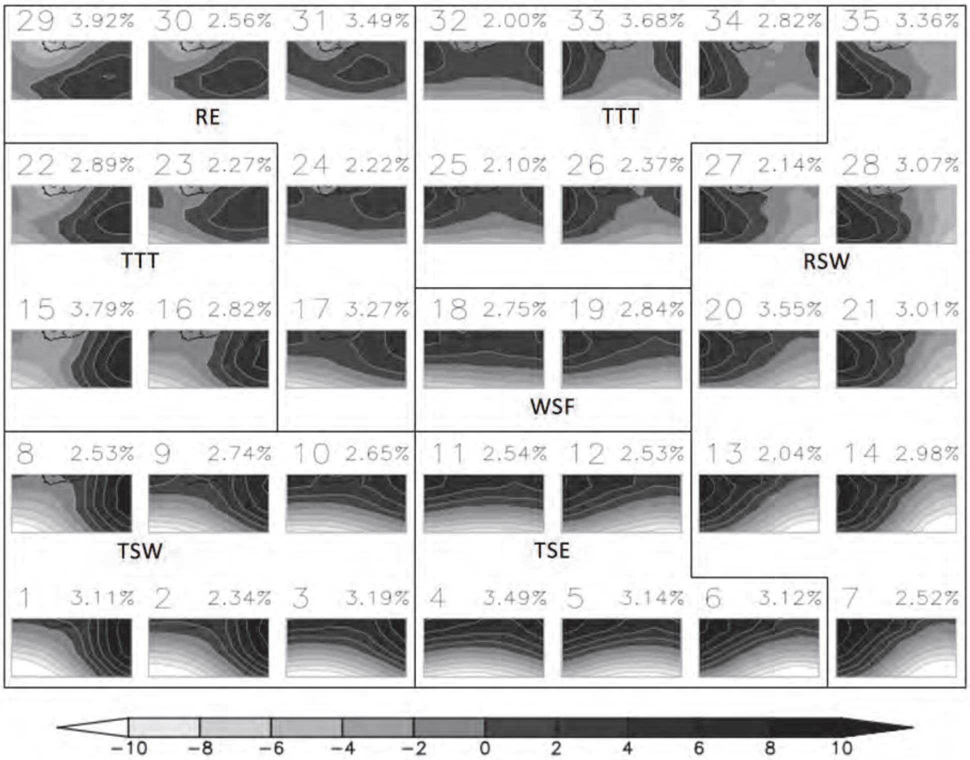

Figure 3.5 SOM of SLP anomalies (hPa) based on daily NCEP reanalysis data from 1979 to 2011. Anomaly SLP contour interval is 2 hPa. Light and dark shades represent negative and positive SLP anomalies, respectively. The node numbers as well as the node frequency of occurrence are indicated on the figure. For the purpose of discussion, the nodes are grouped into the following main synoptic types as indicated: troughs southwest of the subcontinent (TSW), troughs southeast of the subcontinent (TSE), tropical-temperate troughs (TTT), ridging east/southeast of the subcontinent (RE), ridging from southwest of the subcontinent (RSW) and weak synoptic flow (WSF). A detailed discussion on the grouping of nodes can be found in Engelbrecht and Landman, 2015.

On a SOM, similar synoptic patterns are grouped together with nodes characterized by very different patterns being further apart. Generally, the lower part of the SOM is occupied by circulation patterns typical of winter, the upper part by circulation patterns typical of summer and the central part by circulation patterns occurring throughout the year. The spatial rainfall distribution associated with the SOM nodes, represented by composites derived from FEWS data and expressed as mm/day, is shown in Figure 3.6. The synoptic patterns differentiate between distinct rainfall patterns, including rainfall maxima over the Southwestern Cape (e.g. nodes 1-5) tropical-temperate rainband events (e.g. nodes 22, 23, 26, 33), rainfall maxima over the east coast (e.g. nodes 27, 28, 35) and typical summer convection over central and eastern South Africa (e.g. nodes 17-19).

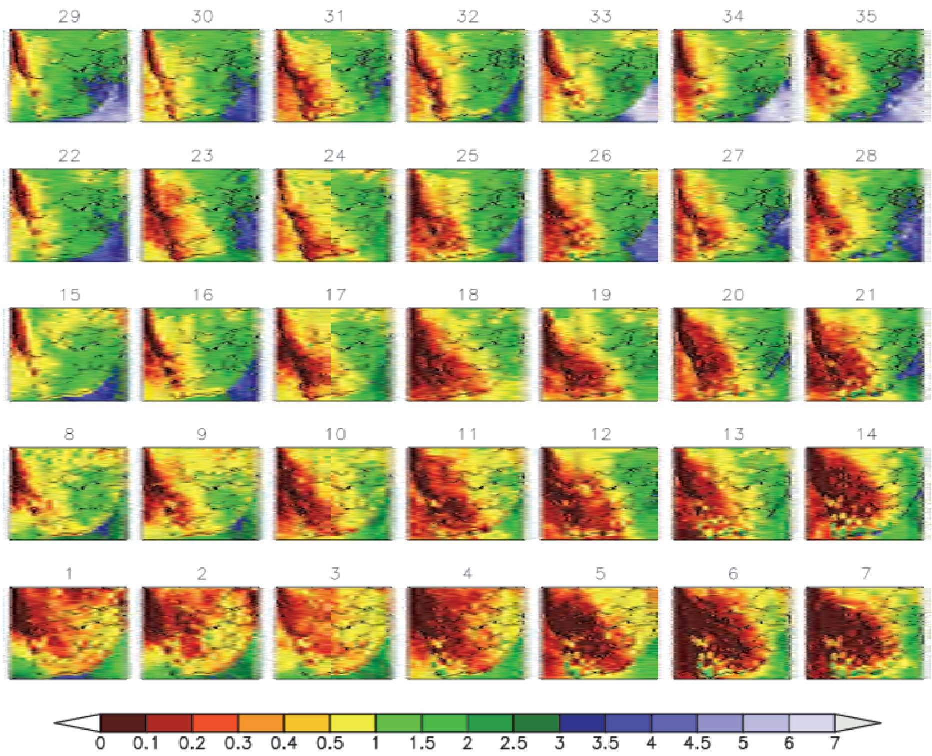

Figure 3.6 Rainfall composites expressed as mm/day derived from FEWS data for the period 1983-2011 for each of the SOM nodes as seen in Fig. 3.5.

The nodes that occur most frequently during each month of the year may be discerned from analysis presented in Figure 3.7. The circulation patterns represented in the lower left corner of the SOM (Fig. 3.5) are strong frontal troughs that occur most frequently during June to August (Fig. 3.7g, h, i). For September (Fig. 3.7j), the nodes occurring most frequently are placed in the lower right corner of the SOM. Here, the paths of the frontal troughs are displaced slightly polewards compared to the winter tracks, allowing for the Atlantic Ocean High (AOH) to extend a ridge along the southern coastal belt of the subcontinent, mainly overland. At the start of the summer season (Fig. 3.7k, l) and during December (Fig. 3.7a), ridging high pressure systems from the southwest ridge from further south (nodes middle and upper right part of the SOM) as the frontal troughs continue to be displaced polewards, with a cell of high pressure moving eastwards to be situated southeast of the subcontinent (upper left corner of the SOM). For January, February and March (Fig. 3.7b, c, d), the nodes in the upper part of the SOM represent the dominant synoptic types. These nodes are representative of the various configurations of tropical-temperate troughs, transforming to tropical-temperate linkages over the western interior during April (Fig. 3.5 node 15, Fig. 3.7e). By May (Fig. 3.7f), the nodes representative of frontal troughs that have migrated equatorward after the summer months, are becoming more frequent again.

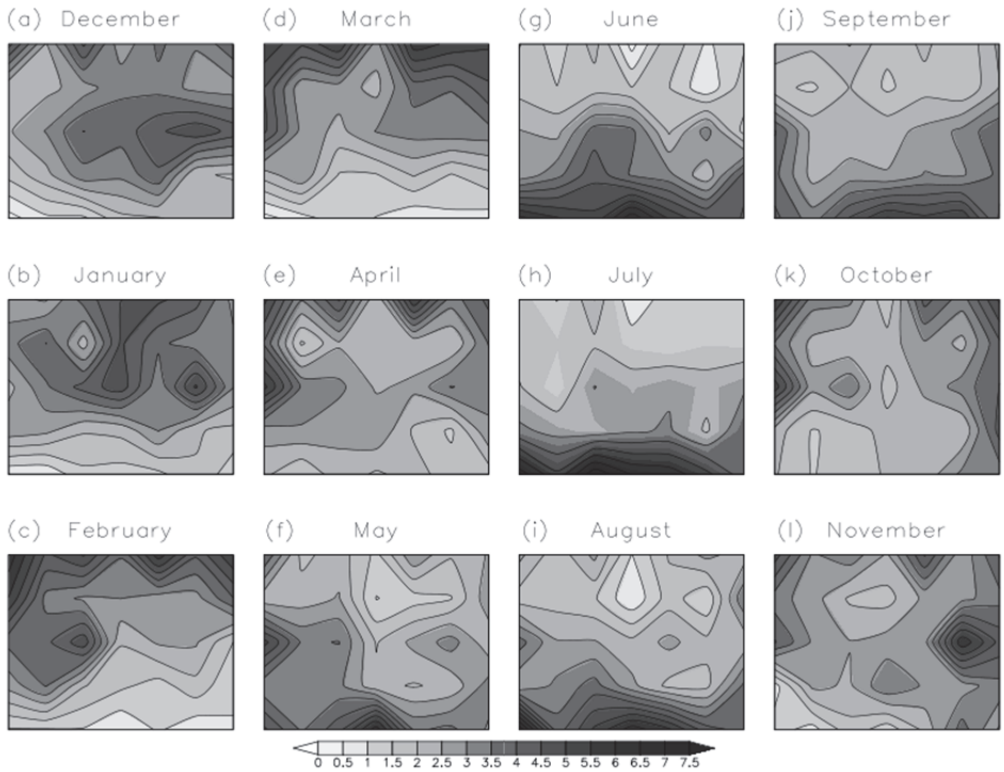

Figure 3.7 Node frequencies (%) for (a) December (1023 days), (b) January (1023 days), (c) February (932 days), (d) March (1023 days), (e) April (990 days), (f) May (1023 days), (g) June (990 days), (h) July (1023 days), (i) August (1023 days), (j) September (990 days), (k) October (1023 days) and (l) November (990 days) that map to each node based on the total days of the particular month from 1979-2011.

3.4 Relating rainfall to the identified synoptic types

To relate rainfall to the main synoptic types identified by the SOM, daily rainfall data (1979-2011) for weather stations in the Cape south coast region were mapped to the SOM. That is, for each day in the time series the relevant circulation pattern may be associated with one of the SOM's synoptic types (e.g. Tennant, 2003). The corresponding daily rainfall totals are subsequently associated with the relevant synoptic type, on a station-by-station basis. This enables calculating the percentage of annual rainfall associated with a specific synoptic type for each station in the region. The percentage contribution by each node to the annual rainfall was calculated by averaging the percentage contributions to rainfall recorded at each of the weather stations (Fig. 2.2) in the all-year rainfall region.

3.5 Relative contribution of synoptic types to rainfall

The percentage contributions of each node to the monthly and seasonal rainfall over the all-year rainfall region are shown in Fig. 3.8 and Fig. 3.9 respectively. The COLs identified by the tracking algorithm were mapped to the relevant node of the SOM for inclusion in the analysis with regards to the relative contribution of the synoptic types to the monthly and seasonal rainfall over the all-year rainfall region (Fig. 3.10). During 1979-2011, 222 COL events (511 COL days) were associated with rainfall over the all-year rainfall region. COL-induced rainfall over the all-year rainfall region is mostly associated with COLs located over the southwestern interior and over the ocean to the west of the country (Fig. 3.10).

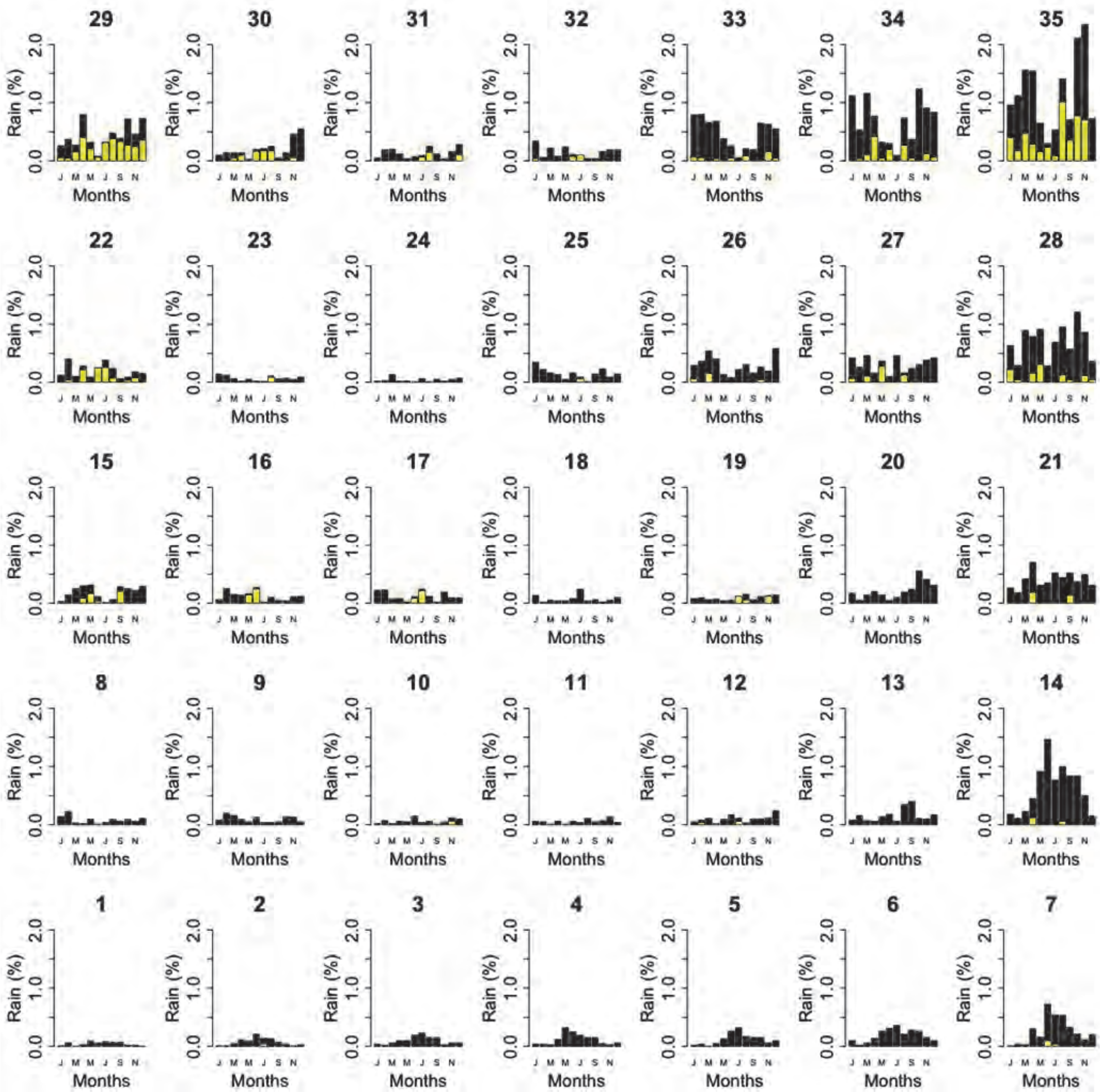

Figure 3.8 Percentage contributions of monthly rainfall totals to the average annual rainfall for each of the nodes. The rainfall contribution associated with COLs is indicated in yellow.

Nodes (or synoptic types) in the upper right part of the SOM are responsible for a relatively large contribution to the annual rainfall as seen in the monthly (Fig. 3.8) and seasonal breakdown (Fig. 3.9). These nodes are typical of the late summer months, February and March (Fig. 3.7). The six nodes in the upper right corner are responsible for 43% of the annual rainfall, while the frequency of occurrence of these nodes is only 17% (Fig. 3.5). These nodes represent the AOH that extends a ridge eastwards at about 40˚ S (nodes 27, 28, 35), as well as tropical-temperate troughs (nodes 26, 33, 34). Node 35 is associated with the largest average daily rainfall. It also has a significantly higher than average occurrence, which in combination with the high average daily rainfall totals lead to this node being associated with 13% of the annual rainfall. It may further be noted that this node is associated with the second highest frequency of COL days associated with rainfall over the region (Fig. 3.10). Node 14 (Fig. 3.5) is also associated with high average daily rainfall totals and has a maximum frequency of occurrence during winter (Fig. 3.7), and represents a high pressure system ridging behind a frontal system that is situated southeast of the subcontinent.

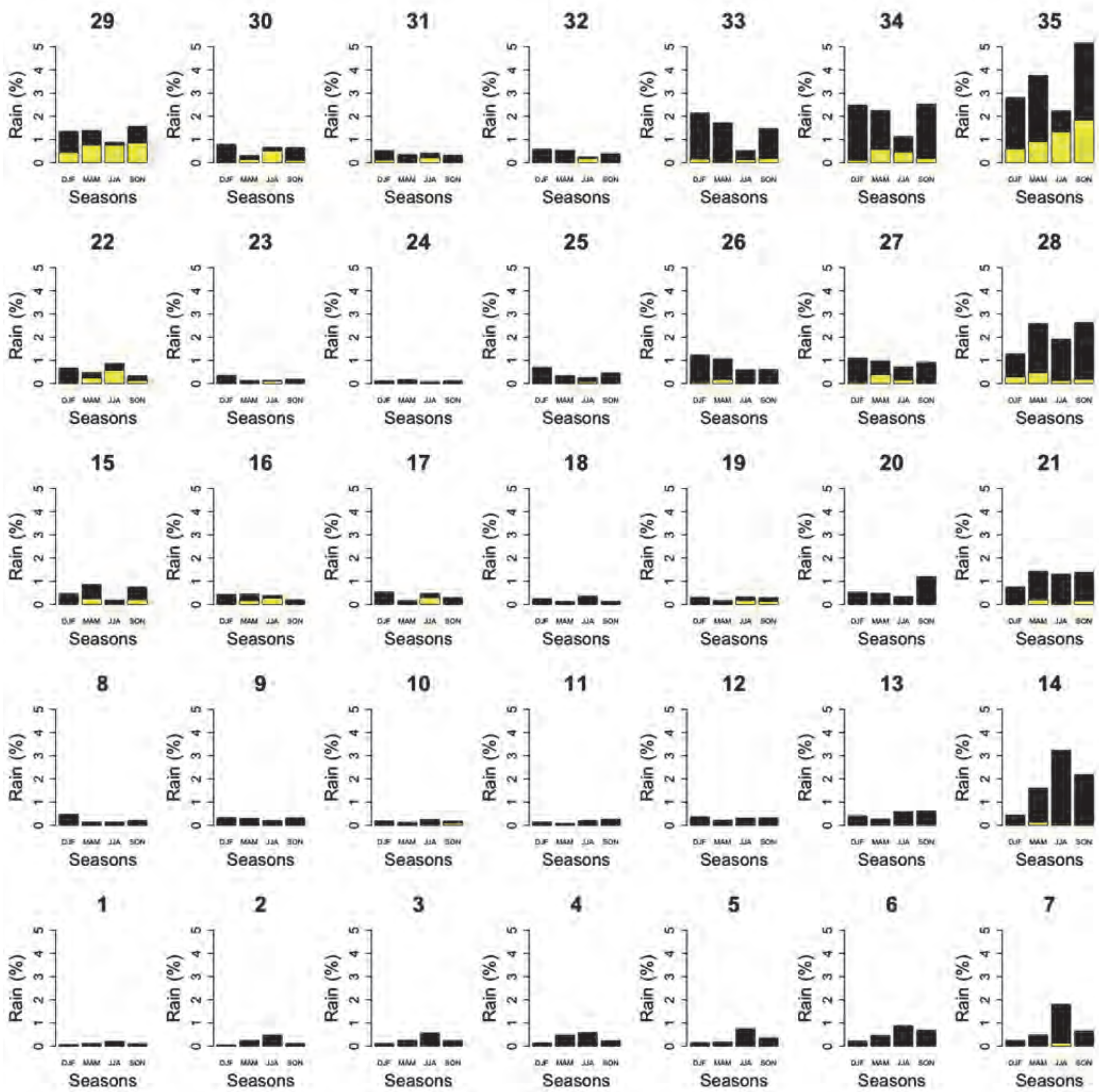

Figure 3.9 Percentage contributions of seasonal rainfall totals to the average annual rainfall for each of the nodes. The rainfall contribution associated with COLs is indicated in yellow.

The nodes representative of frontal troughs located in the lower and middle central part of the SOM, are generally associated with small average daily rainfall totals, and consequently with the smallest contribution to the annual rainfall as revealed by the monthly (Fig. 3.8) and seasonal (Fig. 3.9) rainfall contribution breakdown.

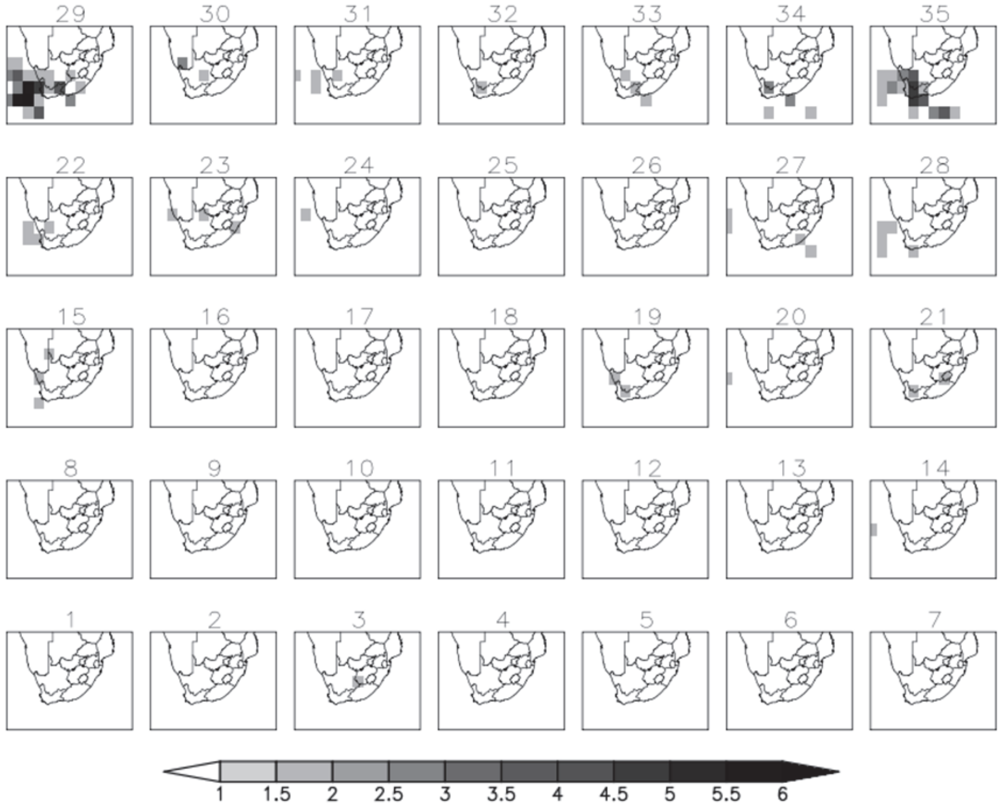

Figure 3.10 Accumulated frequency of rainfall-producing COLs (units: COL days/grid point) for each SOM node for the period 1979-2011. Only grid points with a frequency of at least 1 day are indicated.

From Fig. 3.8 and Fig. 3.9, it can be seen that synoptic systems representative of high pressure systems ridging from the southwest (Fig. 3.5, e.g. nodes 14, 28 and 35) contribute most to rainfall over the all-year rainfall region. Node 35 is associated with COLs, in particular during winter and spring. It is likely though, that the remaining cases are often associated with other forms of upper-air support (e.g. upper air troughs). Still, this result is indicative that the low-level flow around favourably positioned near-surface highs, and possible interactions with the mountainous topography adjacent to the coastal area, are factors of key importance in causing rainfall over the Cape south coast region. The overall contribution of COLs to annual rainfall over the Cape south coast is 16%, much less than the contribution of 39% of ridging highs (nodes 7, 13, 14, 20, 21, 27, 28 and 35) that occur in the absence of COLs. Over the all-year rainfall region, the contribution of COLs to annual rainfall ranges between 13% and 22%. Favre et al. (2013) have found the contribution of COLs to annual rainfall over the Cape south coast to be somewhat higher – in the order of 20 to 30%. Taking into account that only a small number (7 on the average) of COLs contribute to rainfall over the Cape south coast per year, the relatively large portion of rain these systems contribute to the annual rainfall is quite noteworthy. Not surprisingly, when extreme daily rainfall for each station are considered, defined here as the 95th percentile of all recorded rain days, the contribution of COLs to extreme rainfall exceeds that of the contribution of COLs to annual rainfall at all the weather stations over the study region.

The statistics for the nodes associated with the highest average daily rainfall, the highest average contribution to annual rainfall as well as the nodes contributing > 5% each to average annual rainfall are summarized in Table 1.

Table 1 Synoptic types most important to rainfall over the Cape south coast and adjacent interior

Synoptic type rainfall attributes	All-year rainfall region
Highest average daily rainfall	35 (8.4 mm/day)
Highest average contribution to annual rainfall	35 (13%)
Nodes contributing > 5% each to average annual rainfall (ranked according to contribution)	35, 28, 34, 14, 33, 21

3.6 Synoptic types driving the annual rainfall cycle over the Cape south coast

The decomposition of the synoptic types responsible for rainfall over the Cape south coast performed in the previous section shows the relative importance of ridging high pressure systems, tropical-temperate troughs and COLs over this region. The role that each of these systems play in the annual rainfall cycle over the region will subsequently be discussed. Of particular interest is the role of COLs and their association with the observed rainfall peaks (Fig. 2.3), since COL occurrences over South Africa reach maximum numbers during March-May and October (Singleton and Reason, 2007b; Favre et al., 2013), corresponding with two of the three rainfall peaks observed over the Cape south coast region. Moreover, COLs are associated with significant rainfall events along the Cape south coast region (e.g. Taljaard, 1985; Singleton and Reason, 2006; Singleton and Reason, 2007a). In order to investigate the relative contribution of COLs to the rainfall cycle over the Cape south coast, the percentage contribution of COLs to monthly rainfall totals is investigated.

Over the 33-year period analysed, 222 rain-producing COLs occurred that were associated with rainfall over the study region. The preferred geographical location of these COLs is the southwestern interior of South Africa and adjacent oceanic area off the west coast (Fig. 3.10). This region has been identified by Favre et al. (2013) as being one of the areas of southern Africa with the highest frequency of COLs. Autumn (March-May) and winter (June-August) have the highest frequency of occurrence of COLs over the study region, with the highest frequencies in April, May and June (Fig. 3.11).

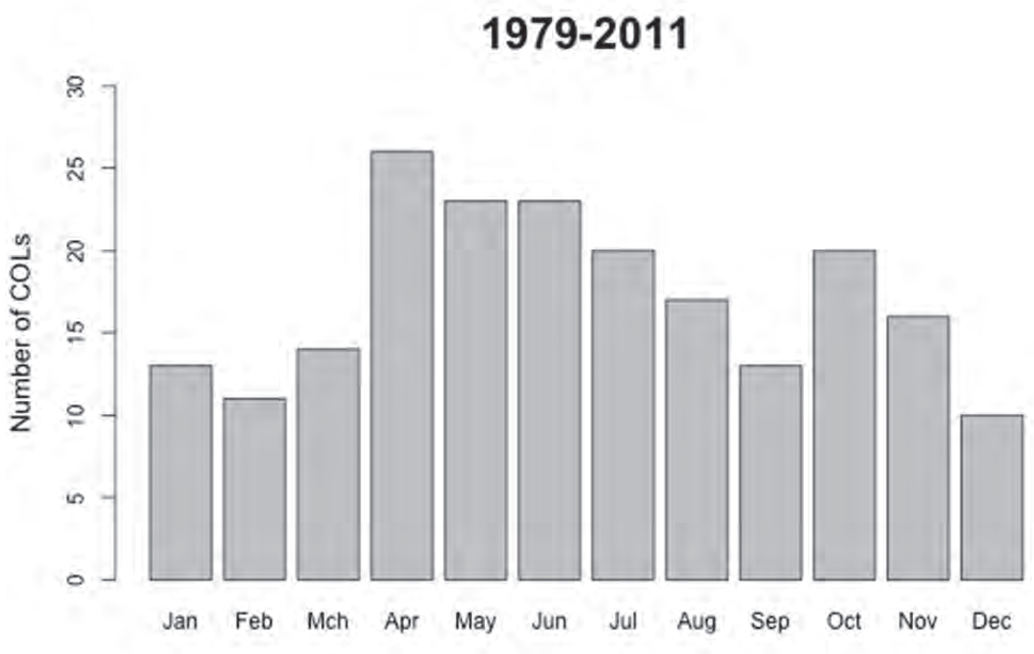

Figure 3.11 Accumulated monthly number of COLs associated with rainfall at 1 station or more, over the period 1979-2011.

Synoptic types associated with the March-April rainfall peak (Fig. 3.12) include troughs, ridging high pressure systems and tropical-temperate troughs, with nodes 21, 26, 27, 28, 33, 34, 35 being the most prominent in contributing rainfall during March, and nodes 7, 14, 21, 26, 28, 29, 33, 34, 35 the most prominent during April (Fig. 3.8). Ridging high pressure systems and tropical-temperate troughs accompanied by COLs contribute to the March rainfall peak while the April rainfall peak is dependent on the contribution by COLs (Fig. 3.12). During March, COLs occur in combination with ridging high pressure systems from the southwest and tropical-temperate troughs (represented by nodes 26, 27, 34 and 35) (Fig. 3.8). The COL-induced rainfall peak during April is characterized by low-level circulation representative of ridging high pressure systems from the southwest and- southeast as well as tropical-temperate troughs – nodes 14, 21, 22, 28, 29, 34 and 35 are representative of the aforementioned synoptic types (Fig. 3.8).

During August, COLs associated with nodes 29 and 35 (Fig. 3.8) are significant contributors to the rainfall peak. Other notable contributions to the rainfall peak are made by ridging high pressure systems (nodes 7, 14, 21, 28) and tropical-temperate troughs (node 34) (Fig. 3.8 and Fig. 3.12).

The month of October is characterized by a prominent rainfall peak over the Cape south coast, and strong rises in the monthly rainfall totals compared to the September total (Fig. 3.12). However, Figure 3.12 also reveals that COL-induced rainfall doesn't peak or rise significantly relative to September totals during October. Ridging high pressure systems from the southwest (nodes 14, 20, 28, 35), tropical-temperate troughs (nodes 33, 34) and high pressure systems southeast of the subcontinent (node 29) are associated with the October rainfall peak (Fig. 3.8). Of these weather systems, ridging high pressure systems from the southwest are responsible for the largest contribution to the rainfall peak. COLs also contribute to the relatively high rainfall totals over Region 1 in November (Fig. 3.12). November is the month with the highest frequency of tropical-temperate troughs over South Africa (Hart et al., 2013).

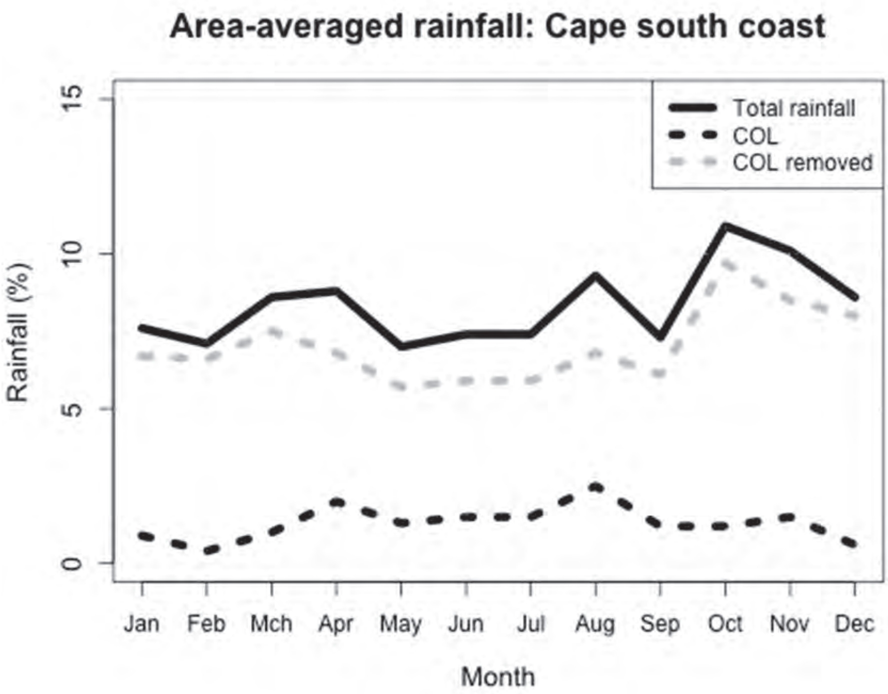

Figure 3.12 Area-averaged annual rainfall distribution for the period 1979-2011 over the all-year rainfall region. The black solid line represents the monthly rainfall (%), the black dotted line the monthly rainfall associated with COLs (%) and the grey dotted line the monthly rainfall without the COL-induced rainfall (%).

3.7 Summary

Ridging high pressure systems are the synoptic types that contribute most to rainfall totals over the Cape south coast region. These systems have a frequency of occurrence of 23% (of the total number of daily occurrences of synoptic types) but contribute 46% of the total rainfall over the Cape south coast. Tropical-temperate troughs are responsible for 28% of the rainfall. The frequency of occurrence of the various configurations of tropical-temperate troughs accumulates to 25%. COLs occur in combination with ridging high pressure systems (ridging from the southwest and southeast) and tropical-temperate troughs. However, the contribution to rainfall by COLs has been isolated from these systems for comparison purposes using an objective tracking algorithm. COLs contribute 16% (7% in co-occurrence with ridging highs). The contribution to rainfall by COLs is remarkable, considering that the COL-induced rainfall days over the Cape south coast region amount only to 4.2%. Transient frontal troughs were found to bring the least rain of the rain-bearing systems, consistent with the observations of the winter months being associated with a season characterized by lower rainfall totals compared to transitional seasons.

The autumn and August rainfall peaks observed in the annual rainfall cycle over the Cape south coast cannot be attributed to a single rain-producing synoptic type. Both ridging highs, tropical-temperate troughs and COLs have been shown to contribute to these rainfall peaks, but with COLs driving the rainfall peak during April. The September hiatus in rainfall that occurs after the August peak, seems to be related to a poleward displacement of frontal systems and positioning of high pressure systems (ridging mainly over land) that are both unfavorable for rainfall. Along the Cape south coast, the October rainfall peak is the highest rainfall peak observed during the year. This rainfall peak is the result of ridging high pressure systems and to a lesser extent tropical-temperate troughs, with an insignificant contribution by COLs. Noteworthy is the importance of ridging high pressure systems relative to COLs for the existence of the October rainfall peak along the coast.

Chapter 4: Synoptic type characteristics during dry and wet seasons

4.1 Defining wet and dry seasons

The seasons considered here are austral summer, autumn, winter and spring, comprising December to February (DJF), March to May (MAM), June to August (JJA) and September to November (SON) respectively. Seasonal rainfall totals for each station (Fig. 2.2) were calculated. The seasonal rainfall totals were spatially averaged and then ranked in order to identify years of above-normal, near-normal and below-normal seasonal rainfall. Thirty-two years of seasonal rainfall totals were considered for each of the four seasons. For each of the seasons the upper-most 10 totals were used to define above-normal rainfall, the 10 lower-most totals define below-normal rainfall and near-normal rainfall is defined by the remaining 12 rainfall totals. The rainfall station data were used to quantify the contribution of COLs to seasonal rainfall totals in order to investigate the role of COLs in interannual variability of seasonal rainfall. Figure 4.1 shows the rainfall totals for 32 DJF (1979/80-2010/11), MAM (1980-2011), JJA (1980-2011) and SON (1980-2011) seasons. A similar analysis at annual time scales is not meaningful, because of a given year having the potential to be wet (or dry), for very different reasons. For example, a year with above-normal rainfall induced by a wet SON will exhibit different synoptic frequencies than a wet year associated with a wet JJA.

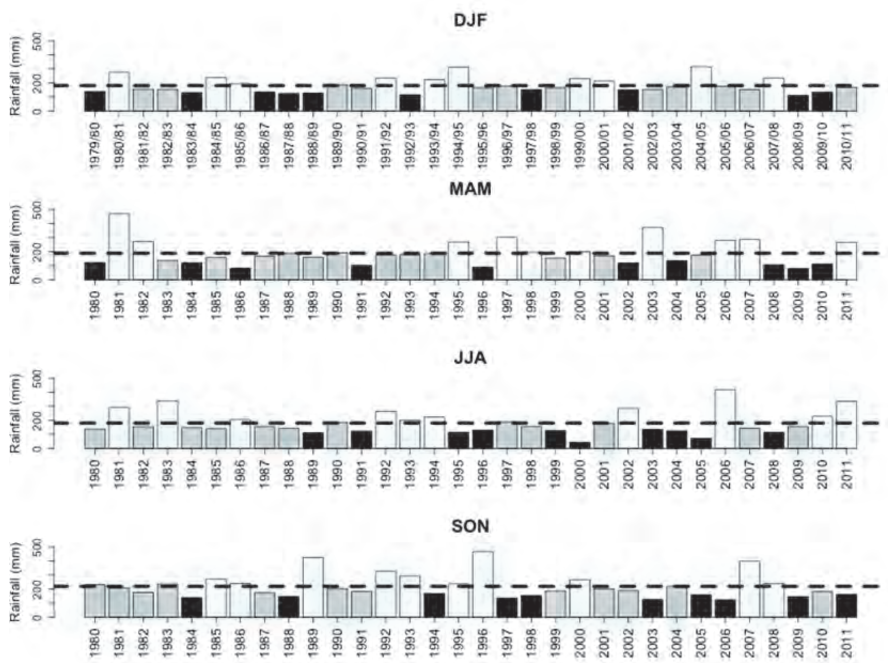

Figure 4.1 The seasonal rainfall (mm) over the Cape south coast for 32 DJF, MAM, JJA and SON years over the period 1979 to 2011. The long-term mean rainfall for each season is indicated by a black dashed line. Seasons of above-normal, near-normal and below-normal rainfall are indicated by light blue, grey and black respectively.

4.2 Seasonal cycle of synoptic types

The seasonal cycle of each node expressed as the percentage occurrence is shown in Figure 4.2. Figure 4.2 is similar to Figure 3.7, but expressed differently for the purpose of highlighting the seasonal cycle associated with each node. Nodes with a strong winter occurrence are observed in the bottom row of the SOM (nodes 1 to 6), while nodes occurring most frequently in summer are found in the top row (nodes 29 to 35). The nodes in the top row of the SOM also show a high frequency of occurrence during the transitional seasons, autumn and spring. However, the highest frequency of occurrence during autumn is found over the left-central part of the SOM (node 15) representative of a surface trough over the far western part of the country linking up with a westerly trough to the southwest of the subcontinent (Fig. 3.5). During spring, nodes located over the right-central part of the SOM (in particular node 21), representative of ridging high pressure systems, exhibit the highest frequency of occurrence. The various configurations of winter frontal systems are represented by nodes 1 to 6. Frontal systems without a pronounced winter occurrence, e.g. represented by nodes 8 and 9, are characterized by a weaker pressure gradient than frontal systems with a strong winter occurrence, e.g. nodes 1 and 2. The frontal systems characterized by stronger pressure gradients are the synoptic types contributing least to annual rainfall over the Cape south coast (Engelbrecht et al., 2015), while these systems are the important rain-producing systems over the winter rainfall region (Lennard and Hegerl, 2015). Ridging high pressure systems and tropical-temperate troughs, found in the top right part of the SOM (nodes 27, 28, 33, 34 and 35), are major contributors to annual rainfall over the Cape south coast (Engelbrecht et al., 2015). Noteworthy is that these systems sometimes co-occur with COLs (Engelbrecht et al., 2015). Nodes representative of synoptic types that occur throughout the year, but lacks evidence of a preferred season of occurrence, are found in the central part of the SOM (Fig. 4.2), and are in general insignificant with regard to annual rainfall contribution over the region (Engelbrecht et al., 2015).

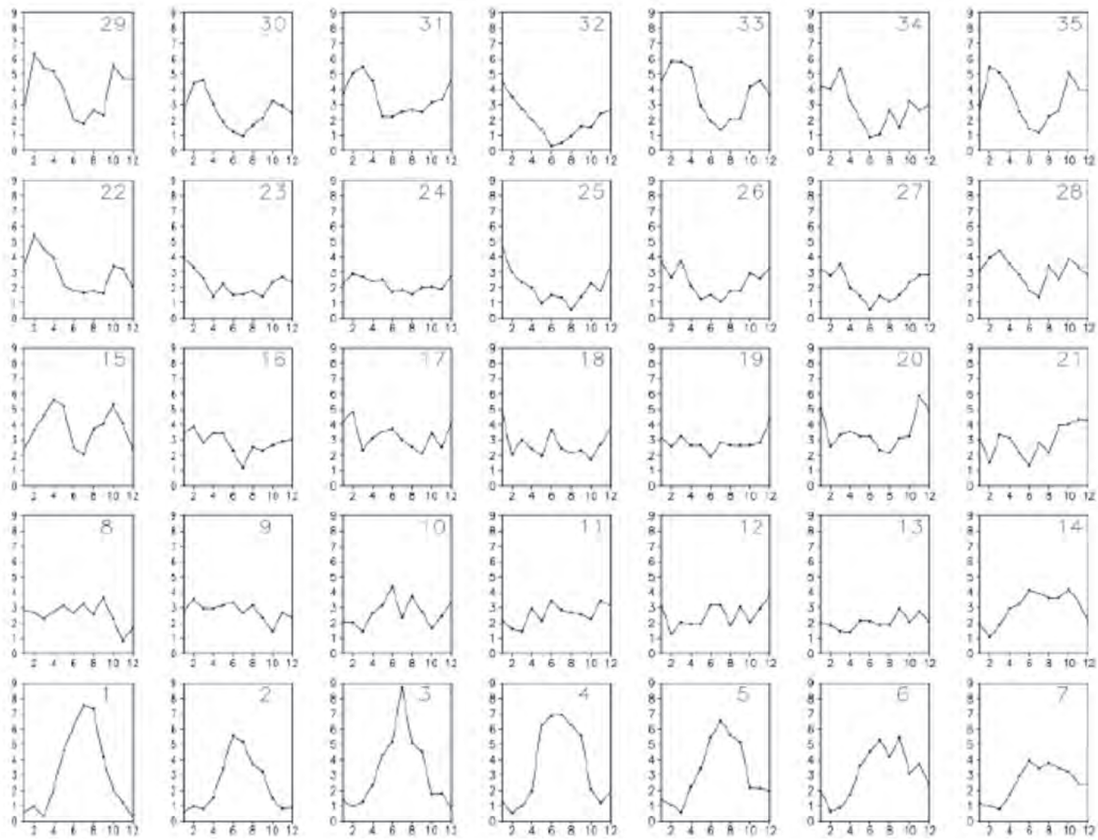

Figure 4.2 Annual cycle (months indicated on the x-axis) of the percentage occurrence (y-axis) for the synoptic types identified by the SOM (node number indicated in the top-right of each panel).

4.3 Circulation anomalies during seasons of anomalous rainfall

Circulation anomalies associated with wet and dry seasons are presented in terms of the frequency of synoptic archetypes occurring during the relevant wet and dry seasons. Circulation anomalies associated with the SOM-nodes for seasons of above-normal, near-normal and below-normal rainfall are calculated relative to the relevant long-term mean for each of the nodes and are expressed as a percentage change of the actual node value before the relevant individual seasons are averaged for the wet, normal and dry seasons (Fig. 4.3). Rainfall anomalies are presented by using two different anomaly metrics to aid in the interpretation of rainfall characteristics that occur during wet and dry seasons. Figure 4.4 shows the average rainfall anomalies (mm) relative to the climatological value of the actual node for the relevant wet, normal and dry seasons. Figure 4.5 shows the rainfall percentage associated with each SOM-node, averaged for seasons of above-normal, near-normal and below-normal rainfall. Evident from Fig. 4.3 is the contrasting frequency relative to the climatological frequency of synoptic archetypes that occur during seasons of above-normal (Fig. 4.3a, d, g and j) and below-normal (Fig. 4.3c, f, i and l) rainfall. Table 4.1 shows the Kendall's tau rank correlation between the 35 node frequencies associated with above-normal rainfall and the corresponding 35 frequencies associated with below-normal rainfall, for each of the four seasons. The contrasting frequency of occurrence of the synoptic archetypes during wet and dry DJF seasons is significant at the 95 % level of confidence

(Kendall's tau rank correlation) while differences in the synoptic archetype frequencies between wet and dry MAM and JJA seasons are significant at the 90 % and 99 % level of confidence (Kendall's tau rank correlation) respectively (Table 4.1). The Pearson product-moment correlation coefficients suggest for this relationship to be linear, in particular for JJA (not shown). Interesting to note is that such a reserved symmetry in terms of the frequency of synoptic archetypes does not exist for dry and wet SON seasons (Table 4.1), although synoptic archetype frequencies differ significantly between dry and normal SON seasons (not shown). The rainfall anomalies (Fig. 4.4) mirror the corresponding circulation anomalies (Fig. 4.3) with regard to the sign of the anomaly, illustrating the link between the total rainfall and the frequency of synoptic types, which suggests that the frequency of occurrence of these synoptic archetypes plays a role in determining whether seasons are dry/wet. The percentage rainfall associated with each node in the SOM during wet and dry seasons (Fig. 4.5) reveals further that the nodes associated with rainfall are very similar during above-normal (Fig. 4.5a, d, g and j), near-normal (Fig. 4.5b, e, h and k) and below-normal (Fig. 4.5c, f, i and l) rainfall seasons. Circulation anomalies during seasons of near-normal rainfall are characterized by a mixture of circulation anomalies that also occur during wet and dry seasons.

Table 4.1 Kendall's tau rank correlation between the frequency of synoptic archetypes during seasons of above-normal versus seasons of below-normal rainfall (see Fig. 4.3), where * = 90 % level of confidence, ** = 95 % level of confidence and *** = 99 % level of confidence

DJF	**MAM**	**JJA**	**SON**
-0.26 **	-0.208 *	-0.415 ***	-0.0605

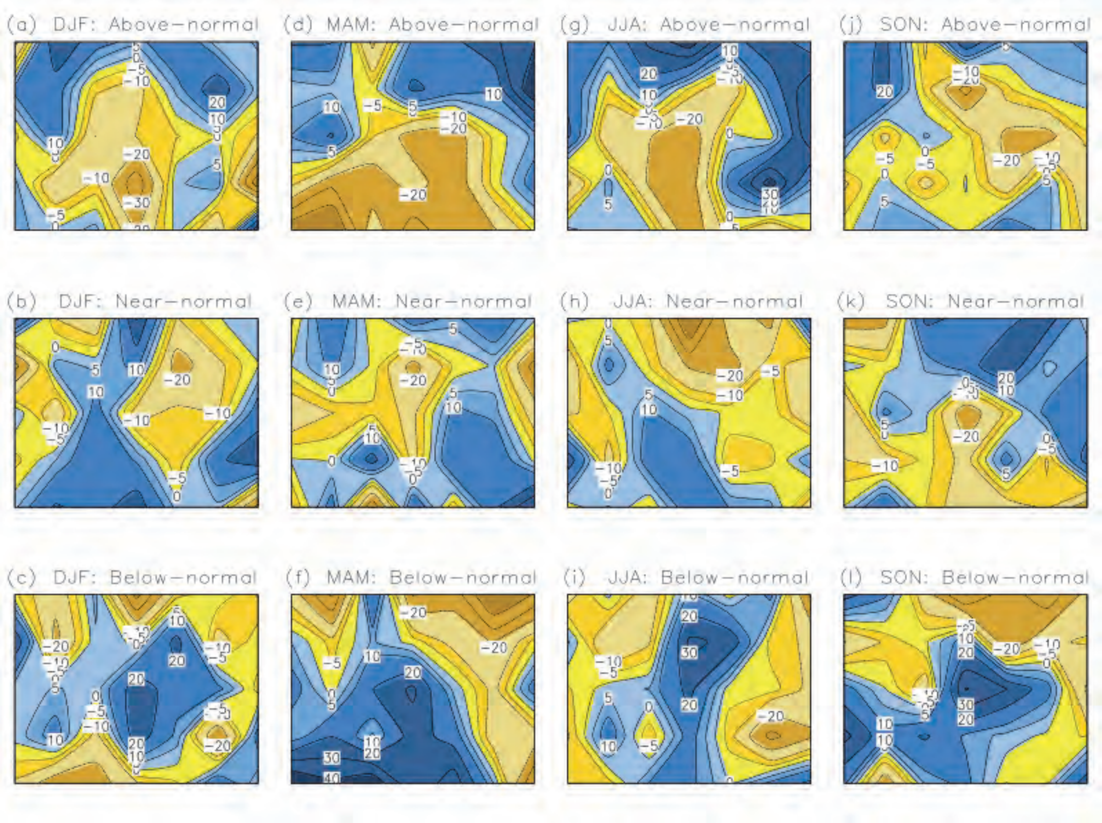

Figure 4.3 Average circulation anomalies for seasons of above-normal (top row), near-normal (middle row) and below-normal (bottom row) rainfall as represented by the SOM-node frequency expressed as a percentage change for each of the nodes relative to the relevant long-term mean frequency of the relevant SOM-node. Positive (negative) anomalies are indicated by blue shades (yellow shades).

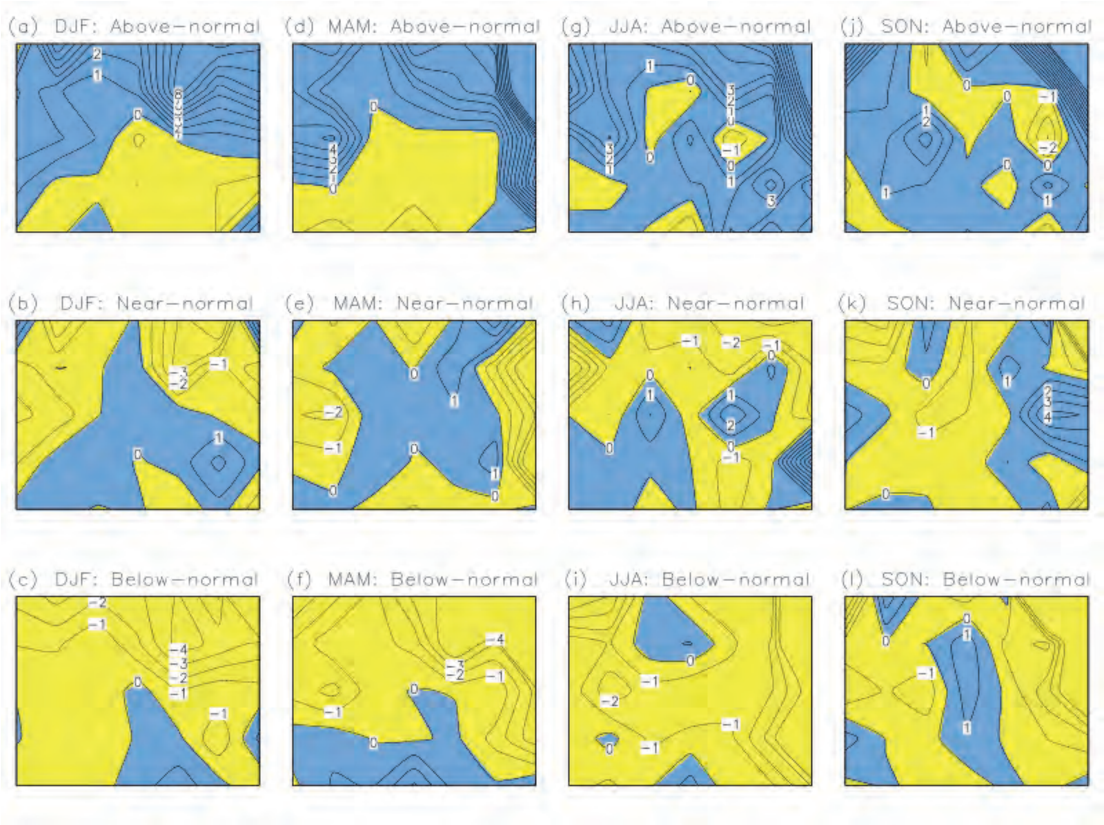

Figure 4.4 Average rainfall anomalies (mm) for seasons of above-normal (top row), near-normal (middle row) and below-normal (bottom row) rainfall as represented by the rainfall associated with each of the nodes relative to the relevant long-term mean rainfall of the relevant SOM-node. Positive (negative) anomalies are indicated in blue (yellow).

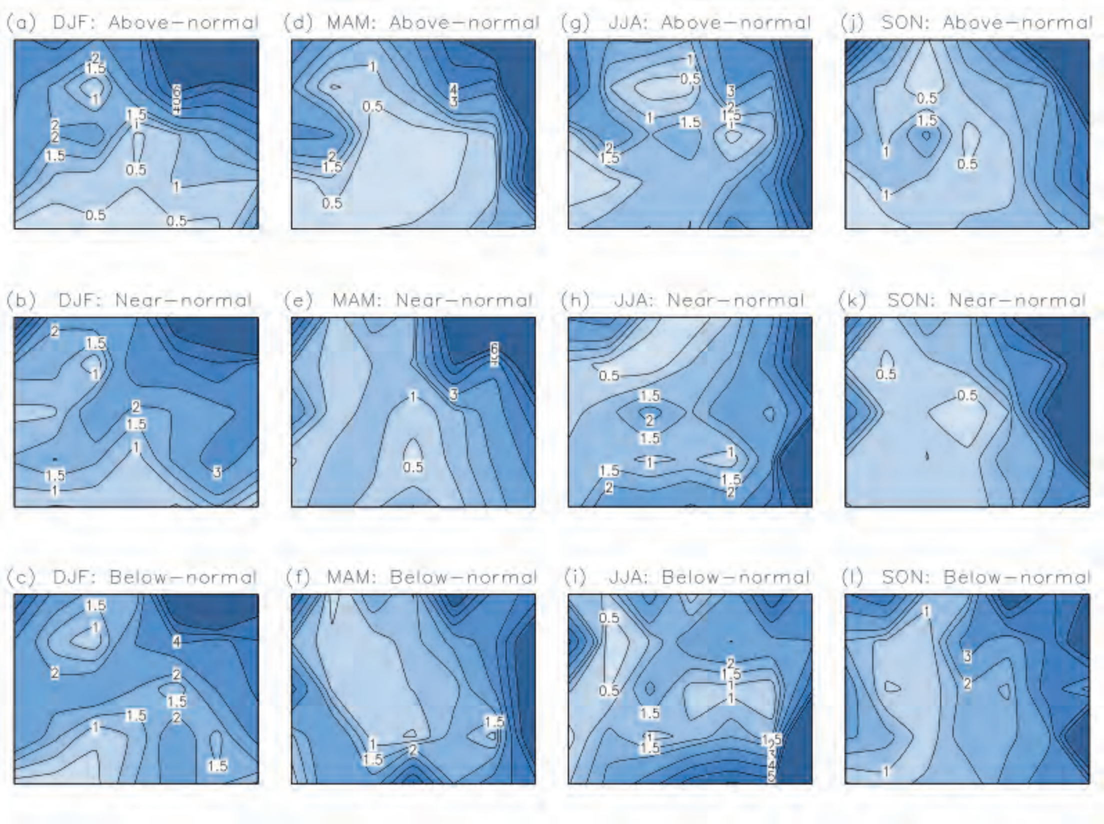

Figure 4.5 Average percentage of rainfall for the SOM-nodes associated with seasons of above-normal (top row), near-normal (middle row) and below-normal (bottom row) rainfall.

4.4 Synoptic type rainfall and interannual variability of seasonal rainfall

Climatological seasonal rainfall totals over the Cape south coast are very similar (Table 4.2). Rainfall-producing synoptic types with an occurrence throughout the year includes ridging high pressure systems from the southwest and COLs while the contribution by tropical-temperate troughs and frontal systems peak during October to April and May to August respectively (Engelbrecht et al., 2015). In the case of ridging high pressure systems, seasonality is observed in the preferred configuration of this synoptic type that contributes to rainfall. For example, ridging high pressure systems from the southwest represented by nodes 7 and 14 are characteristic of winter, while nodes 20, 27 and 35 exhibit summer peaks in their occurrence (Fig. 4.2). Objective 3 of this study is to identify important synoptic types and/or configurations within a specific synoptic type that are linked to interannual variability of seasonal rainfall over the Cape south coast. A direct approach to address this question is to test whether a significant positive correlation exists between the rainfall associated with the synoptic types and the total seasonal rainfall. It is firstly tested whether rainfall associated with nodes representative of a similar synoptic type collectively correlate with seasonal rainfall totals.

Table 4.2 Climatological seasonal rainfall totals (mm)

DJF	MAM	JJA	SON
181	189	181	219

During DJF and MAM, rainfall associated with ridging high pressure systems from the southwest, ridges situated east of the subcontinent and tropical-temperate troughs (Table 4.3) exhibit a significant positive rank correlation with the respective seasonal rainfall totals, suggesting that these synoptic types are linked to interannual variability of DJF and MAM rainfall. During JJA and SON, rainfall associated with ridging high pressure systems from the southwest and ridges situated east of the subcontinent exhibit a significant positive rank correlation with JJA and SON rainfall totals respectively (Table 4.3). Ridging high pressure systems from the southwest seem to have the strongest link to interannual variability of seasonal rainfall – significant at the 99 % level of confidence during DJF, MAM, JJA and SON, followed by ridges situated east of the subcontinent (Table 4.3). For the latter, the link to interannual variability seems stronger during DJF and MAM compared to JJA and SON. Pearson product-moment correlation coefficients indicate that this relationship is linear (not shown). Ridging high pressure systems from the southwest show the strongest linear relationship with interannual variability of seasonal rainfall. It may be noted that the maximum COL occurrence co-occurs with nodes within the groups representing ridging high pressure systems from the southwest (Fig. 2, node 35) and ridges situated east of the subcontinent (Fig. 2, node 29) (Engelbrecht et al., 2015). This is likely to influence the positive correlation of these groups with seasonal rainfall totals as COLs are associated with heavy rainfall events (Rouault et al., 2002; Singleton and Reason 2006, 2007a).

Table 4.3 Kendall's tau rank correlation between circulation type seasonal rainfall (mm) and total seasonal rainfall (mm) over the period 1979 to 2011, where * = 90 % level of confidence, ** = 95 % level of confidence and *** = 99 % level of confidence

Grouped synoptic types / main circulation types	**Trough southwest**	**Trough southeast**	**Ridging high pressure**	**Ridge east**	**Tropical-temperate trough**	**Weak synoptic flow**
Nodes	1, 2, 3, 8, 9, 10	4, 5, 6, 11, 12	7, 13, 14, 20, 21, 27, 28, 35	17, 24, 29, 30, 31	15, 16, 22, 23, 25, 26, 32, 33, 34	18, 19
DJF	0.16	-0.19	0.42^{***}	0.33^{***}	0.26^{**}	-0.006
MAM	-0.2	-0.14	0.69^{***}	0.58^{***}	0.32^{**}	-0.06
JJA	0.16	0.07	0.58^{***}	0.28^{**}	0.19	-0.05
SON	-0.05	0.09	0.6^{***}	0.24^{*}	0.17	-0.09

The various configurations within the grouped synoptic types (represented by the individual nodes shown in Fig. 3.5), represent variations of attributes such as geographical and seasonal location, intensity and some structural features. In an attempt to highlight or isolate what specific configuration within a synoptic type is the preferred driver of interannual variability of seasonal rainfall, the seasonal rainfall associated with the individual nodes was also correlated with seasonal rainfall totals (Table 4.4). Noteworthy, is the presence of 2 specific configurations of ridging high pressure systems from the southwest, those with the most southward located axis (Fig. 3.5, nodes 28 and 35), that are correlated with rainfall totals for DJF, MAM, JJA and SON. Ridging high pressure systems from the southwest representative of nodes 28 and 35 are suggested to be a driver of interannual variability of SON rainfall in particular with correlations significant at the 99 % level of confidence (Table 4.4). In the case of the tropical-temperate troughs, a significant correlation with DJF, MAM and SON rainfall totals exists. During DJF, rainfall associated with tropical-temperate troughs with the smallest node-averaged zonal wind component over and to the south of the country (nodes 32) are correlated to DJF rainfall totals, consistent with the jet stream that is located further poleward during years of above-normal rainfall over the summer rainfall region and hence weaker winds (Tennant and Reason, 2005).

During MAM and SON other configurations of tropical-temperate troughs are linked to interannual variability of seasonal rainfall, illustrating the seasonality that can occur within a specific group of synoptic types.

Table 4.4 Nodes for which the node-associated rainfall is significantly correlated with the seasonal rainfall totals over the period 1979 to 2011. Node numbers are indicated in bold. Kendall's tau rank correlation and the significance level is indicated in brackets where * = 90 % level of confidence, ** = 95 % level of confidence and *** = 99 % level of confidence

Seasons	Nodes for which the node associated rainfall is significantly correlated with the seasonal rainfall totals
DJF	**27** (0.27**), **28** (0.23*), **32** (0.3**), **35** (0.22*)
MAM	**2** (-0.3**), **4** (-0.33***), **15** (0.25**), **16** (0.32**), **25** (0.24*), **27** (0.28**), **28** (0.22*), **30** (0.45***), **33** (0.26**), **34** (0.3**), **35** (0.32**)
JJA	**1** (0.25*), **2** (0.22*), **4** (-0.26**), **13** (0.3**), **21** (0.27**), **28** (0.44***), **29** (0.24*), **35** (0.25*)
SON	**8** (-0.29**), **16** (0.24*), **22** (0.22*), **28** (0.38***), **33** (0.24*), **35** (0.4***)

COLs contribute to 16 % of annual rainfall totals, co-occurring with ridging high pressure systems and tropical-temperate troughs (Engelbrecht et al., 2015). The nature of COLs to cause high impact rainfall events that have the ability to produce 24-h rainfall totals that exceed the relevant climatological monthly rainfall (Singleton and Reason, 2006; 2007a; Muller et al., 2008), warrants the consideration of a linkage between COL-induced rainfall and interannual variability in seasonal rainfall. Mean seasonal rainfall totals attributed to COLs are of comparable magnitude for MAM, JJA and SON with mean seasonal total rainfall during DJF only half or less of any of the other seasons (Table 4.5). Over South Africa COLs occur most frequently during MAM (31 %), followed by JJA (29 %), SON (22 %) and DJF (18 %) (Table 4.5), similar to COL seasonal frequencies from Singleton and Reason (2007b) and Favre et al. (2013). The relationship between the frequency of COLs and COL-induced rainfall is not linear. Although spring (SON) has a lower frequency of COLs than autumn (MAM) and winter (JJA), it is the season when the highest percentage of COLs is associated with rainfall over the Cape south coast. Spring, when defined as October-November-December (OND), is also the season when COL-induced rainfall over South Africa is on average widespread (Favre et al., 2013). During winter (JJA), the mean seasonal rainfall attributed to COLs over the Cape south coast is a maximum (38 mm) (Table 4.5). Favre et al. (2013) also identified winter (defined as July-August-September (JAS)) to be the season with the largest contribution to annual COL rainfall. South Africa on average, however, receives the largest contribution to annual COL rainfall during OND (Favre et al., 2013).

Table 4.5 Climatological seasonal statistics for COL induced rainfall in mm (second column), percentage of COL occurrences over South Africa (third column) and percentage of COLs that produce rainfall over the Cape south coast (fourth column)

Attribute	**Long-term average seasonal COL rain (mm)**	**Long-term average seasonal COL distribution over South Africa (%)**	**Long-term average percentage of COLs over South Africa associated with rain over the Cape south coast**
DJF	15.3 mm	18 %	56 %
MAM	33.8 mm	31 %	61 %
JJA	38.4 mm	29 %	63 %
SON	30.6 mm	22 %	68 %

The influence of rainfall associated with COLs on seasonal rainfall totals is shown in Fig. 4.6. A weak and non-significant correlation exists for summer (DJF), the season with the lowest mean frequency of COLs and COL-associated rainfall. Autumn (MAM) and winter (JJA) have the highest and most significant (99 % level of confidence) correlation between COL-associated seasonal rainfall totals and all seasonal rainfall totals. A weak but significant correlation exists for spring (SON) which may be attributed to ridging high pressure systems that contribute largely to October rainfall, the month observed with the highest area-averaged monthly rainfall totals along the Cape south coast (Engelbrecht et al., 2015). The Pearson product-moment correlation coefficients indicate that the relationship between COLs and interannual rainfall variability is linear, in particular for JJA and MAM (not shown). Even though the frequency of occurrence of COLs is low, as illustrated by the absence of a node dedicated only to COLs in the SOM, COLs can have a notable impact on seasonal rainfall totals (e.g. JJA 2006, Fig. 4.6) – an indication of the intensity of COLs.

The geographical location of COLs during wet and dry seasons exhibits different regions of preferred occurrence (Fig. 4.7). The mean COL frequency anomaly for wet DJF seasons is characterized by COLs most frequently located over the western part of the Northern Cape and Southwestern Cape. During MAM, JJA and SON wet seasons are in general characterized by an increase in the frequency of COLs occurring countrywide. Noteworthy are areas of increased COL activity during wet seasons just off the Cape south coast and over the interior to the northwest of the Cape south coast, consistent with increased mid-latitude cyclone system density associated with wet years (Weldon and Reason, 2014). During seasons of below-normal rainfall, the aforementioned areas are generally characterized by a negative mean COL frequency anomaly, consistent with a polewards shift of storm tracks (Weldon and Reason, 2014).

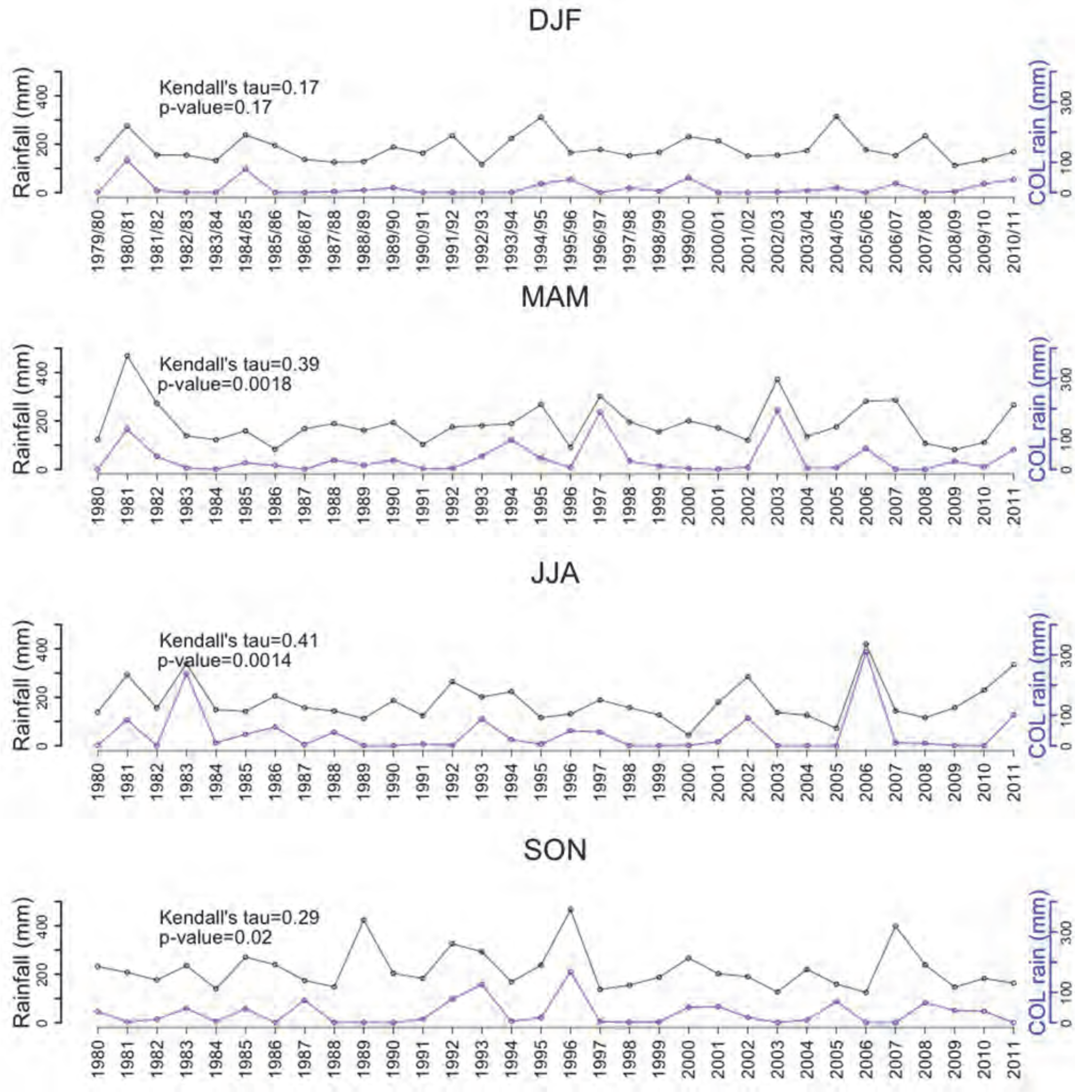

Figure 4.6 Kendall's tau rank correlation between seasonal rainfall totals and the corresponding COL-induced rainfall totals.

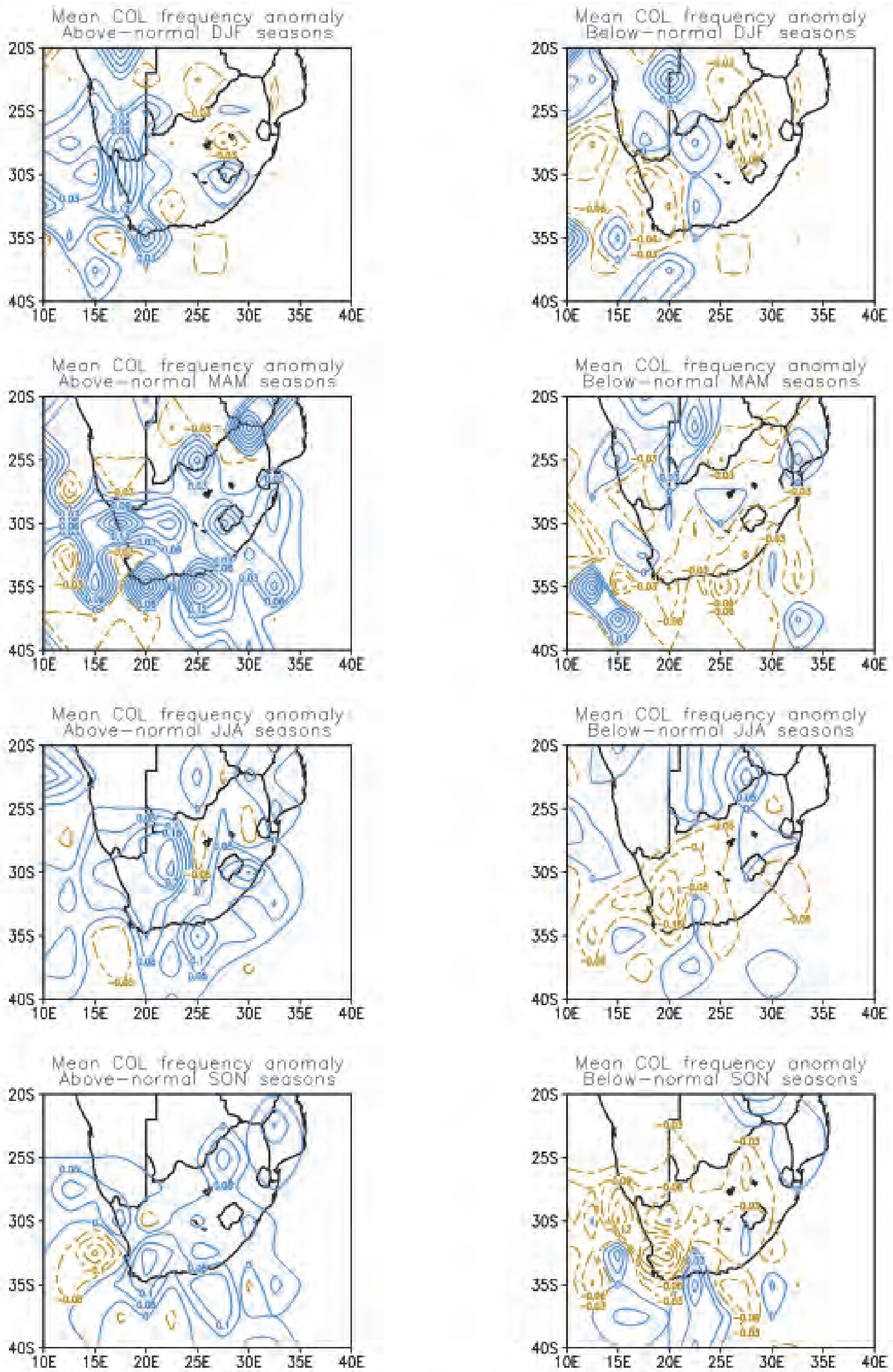

Figure 4.7 Geographic location of COLs (COL centre frequency per grid point) for DJF, MAM, JJA and SON seasons of above-normal (left) and below-normal (right) rainfall relative to the climatological mean of COL centre frequency per grid point.

4.5 Summary

The link between interannual variability of seasonal rainfall over the Cape south coast of South Africa and different synoptic types was explored. Synoptic circulation over the region is classified into different synoptic types by employing a clustering technique, the SOM, on daily circulation data for the 33-year period from 1979 to 2011. Daily rainfall data are used to investigate interannual variability of seasonal rainfall within the context of the identified synoptic types. The anomalous frequency of occurrence of the different synoptic types for wet and for dry seasons differs significantly within the SOM space, except for austral spring. The main rainfall-producing synoptic types are to a large extent consistent for wet and dry seasons. The main rainfall-producing synoptic types have a notable larger contribution to seasonal rainfall totals during wet seasons than during dry seasons, consistent with a higher frequency of occurrence of the main rainfall-producing synoptic types during wet seasons compared to dry seasons. Dry seasons are characterized by a smaller contribution to seasonal rainfall totals by all the different synoptic types, but with the largest negative anomalies associated with low frequencies of the main rainfall-producing synoptic types. The frequencies of occurrence of specific configurations of ridging high pressure systems, cut-off lows (COLs) and tropical-temperate troughs associated with rainfall are positively linked to interannual variability of seasonal rainfall.

Chapter 5: Streamflow and synoptic type association over the all-year rainfall region

5.1 Background

The Cape south coast expierences drought as well as floods from time to time (Taljaard, 1996; Weldon and Reason, 2014). During the 2009 to 2010 drought, local disasters were declared in the George and Knysna Municipalities (Holloway et al., 2012). Reservoir levels declined in response to reduced streamflow and were not able to supply in the daily need of water. The water storage crises were not the result of the meteorological drought alone but were accentuated by the urban growth experienced in the region coupled with limited reservoir capacity (Halloway et al., 2012). On the other extreme, flood events are characterized by an abrupt increase in streamflow to levels that can be disasterous. It has been illustrated that despite the complex association between rainfall and streamflow (Landman et al., 2001b), categorized streamflow prediction on the seasonal timescale over the northeastern part of South Africa can have useful skill (Landman et al., 2001b; Malherbe et al., 2014). These forecasts made use of the relationship between streamflow and atmospheric variability (Landman et al., 2001). In this project, the association between rainfall and circulation patterns has been addressed (Chapters 2, 3 and 4). In this chapter, the aim is to investigate the association between streamflow and specific weather systems (as represented by the 35 nodes as seen on Fig. 3.5) relevant to the all-year rainfall region of South Africa.

5.2 Streamflow characteristics over the all-year rainfall region

Streamflow data were downloaded from the Hydrological Information System data portal (https://www.dwaf.gov.za/hydrology/hymain.aspx) hosted by the Department of Water and Sanitation. Monthly and daily streamflow data were downloaded for river gauge stations in drainage region K as well as for one river gauge station in drainage region M (Table 5.1 and Figure 5.1). The entire draining region K is located within the all-year rainfall region. The eastern extremities of the all-year rainfall region co-incide with drainage region M, except for the extreme northern part of draining region M that recieves mostly summer rainfall. The monthly data were used to calculate mean monthly streamflow for the period from 1979 to 2013. Mean monthly streamflow at various measuring points in drainage region K and for one measuring point in drainage region M are shown in Figure 5.2. Streamflow is fairly evenly distributed between the months except over the far eastern part of drainage region K and at the measuring point in drainage region M where clear peaks occur during some winter and spring months. The peak in streamflow observed during August at measuring points K8H005, K9H001 and K9H003 is striking. At measuring point M1H012 the streamflow peak is observed in October, followed by the month of August. It may be noted that the annual streamflow cycle is very similar to the rainfall cycle observed at rainfall stations.

Table 5.1 Streamflow stations used for calculation of the monthly longterm mean streamflow

River gauge Nr.	Latitude	Longitude	River and measuring point	Catchment area (km^2)	Data period
K1H017	-34.09694	22.01028	Hartenbos River @ Hartebeestkuil	101	1979-2013
K2H002	-34.02861	22.22194	Great-Brak River @ Wolvedans	131	1979-2013
K3H001	-33.93778	22.46083	Rooi river @ George	1.04	1979-2013
K4H003	-33.91250	22.70778	Diep River @ Woodville Forest Res	72	1979-2013
K5H002	-33.89111	23.02944	Knysna River @ Milwood Forest Res	133	1979-2013
K6H001	-33.80361	23.13528	Keurbooms River @ M'Kama	165	1979-2013
K6H019	-33.94583	23.36750	Keurbooms River @ Newlands	N/A	1998-2013
K7H001	-33.95556	23.63861	Bloukrans River @ Lotterings For. Res.	57	1979-2013
K8H001	-33.98194	24.02097	Kruis River @ Farm 508	25.64	1979-2013
K8H005	-34.09664	24.43911	Tsitsikama River @ Geelhoutboom	134	1996-2013
K9H001	-34.00586	24.49914	Krom River @ Kromme Riviers Poort	368.5	1979-2013
K9H003	-34.09583	24.69472	Krom River @ Elandsjagt	844	1984-2013
M1H012	-33.77192	25.38639	Swartkops River @ Uitenhage	912	1995-2013

Figure 5.1 Geographical location of reservoirs (pink), river gauges (yellow) and rivers (brown) over the Cape south coast draped over the topography as represented by the SRTM 90m DEM. Rivers with operational gauges are indicated in blue.

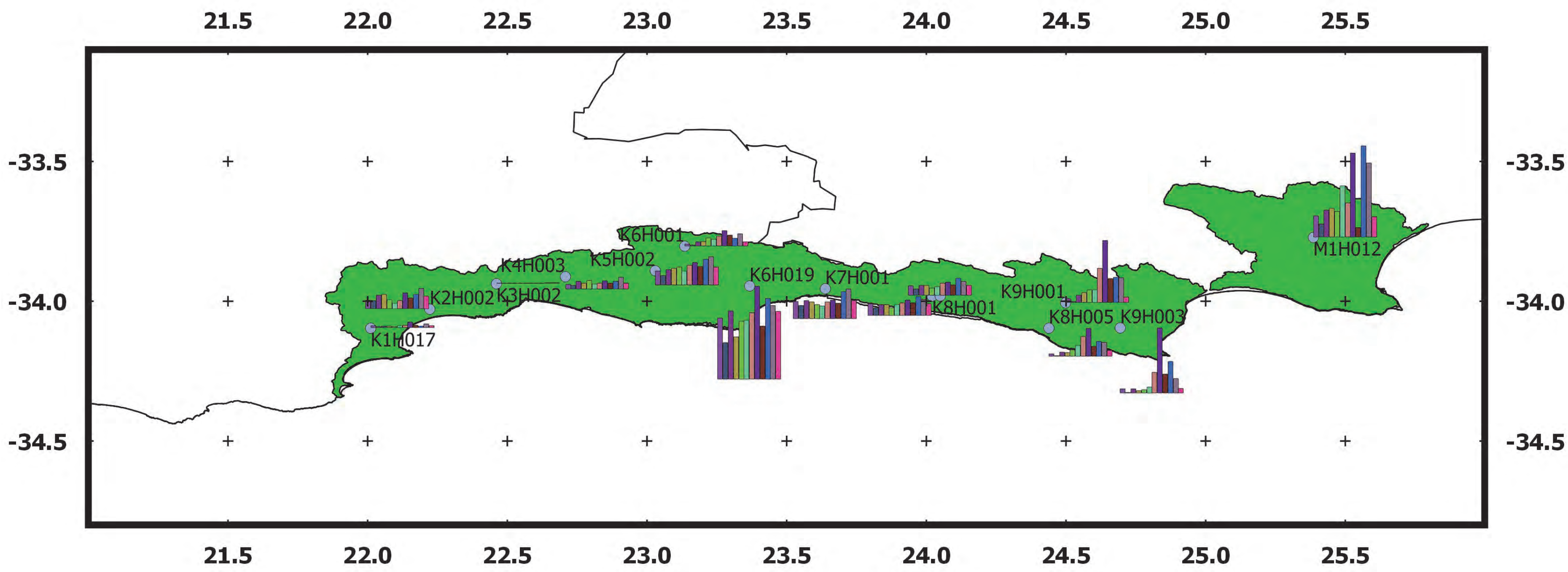

Figure 5.2 Mean monthly streamflow (millions of m^3) measured by river gauges located in drainage regions K and M.

5.3 Association between synoptic types and streamflow

The daily streamflow data were mapped to the identified synoptic types as represented in Figure 3.5 in order to quantify the potential contribution of streamflow associated with each of the weather systems to mean monthly streamflow. This analysis is performed for streamflow measured at selected river guages, namely river guage K4H003, K6H019 and K8H001. These river guages are chosen based on their geographic location that is evenly spread over drainage region K.

Circulation patterns 28 and 35 (representative of strong ridging high pressure systems) and to a lesser extent circulation patterns 14 and 21 (representative of ridging high pressure systems) are associated with the most notable streamflow observed at river gauges K4H003 (Fig. 5.3), K6H019 (Fig. 5.4) and K8H001 (Fig. 5.5). The seasonal distribution of streamflow associated with the different circulation patterns that contributes to the mean annual streamflow is very similar at these measuring points.

Circulation pattern 35 is associated with the largest contribution to mean annual streamflow at the three measuring points discussed above, of which nearly half of this contribution is associated with COLs (Fig. 5.6). Other circulation patterns associated with notable streamflow contributions are circulation patterns 14 (ridge from the southwest), 15 (tropical-temperate trough), 20 (ridge from the southwest), 21 (ridge from the southwest), 27 (ridge from the southwest), 28 (ridge from the southwest), 29 (ridge from the southeast), 30 (ridge from the southeast), 31 (ridge from the southeast), 32 (tropical-temperate trough), 33 (tropical-temperate trough) and 34 (tropical-temperate trough). The COL component of the streamflow contributions associated with the aforementioned circulation patterns are fairly evenly spread for the three river gauges.

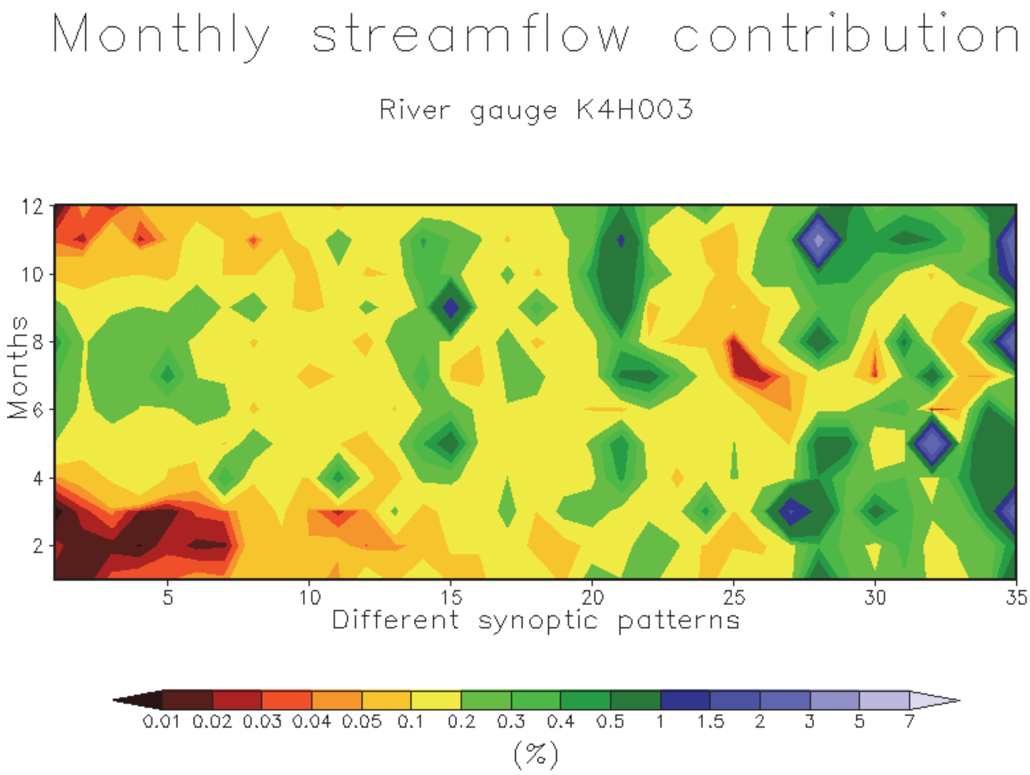

Figure 5.3 Monthly percentage contribution to mean annual streamflow at river gauge K4H003 associated with the different synoptic patterns.

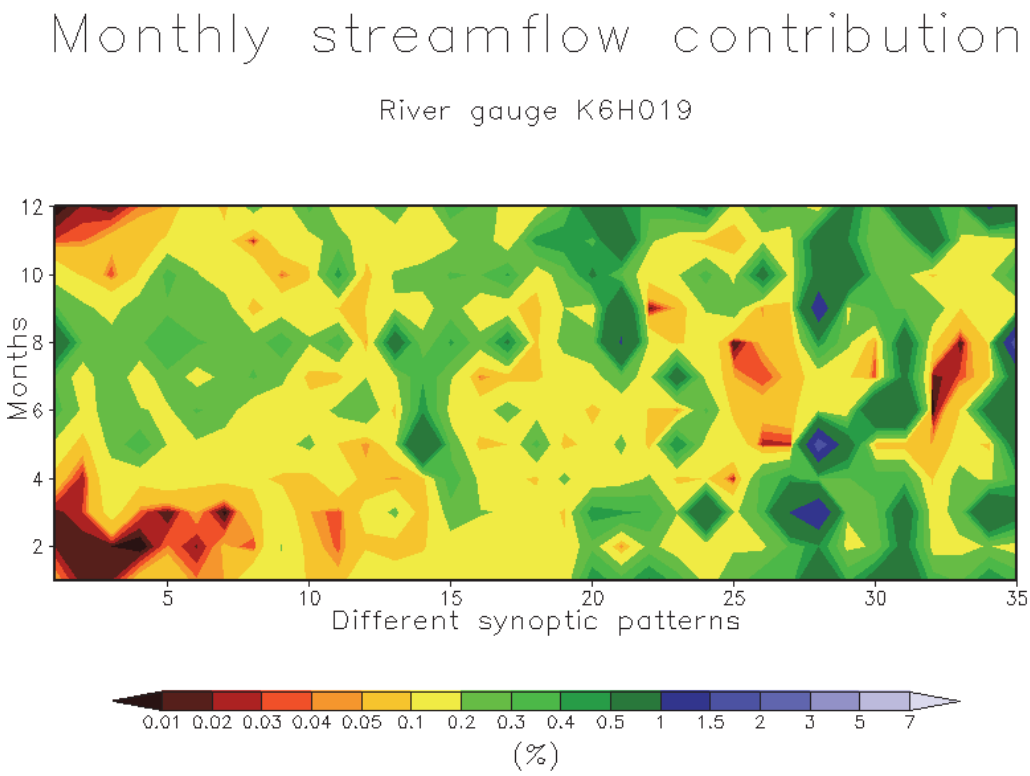

Figure 5.4 Monthly percentage contribution to mean annual streamflow at river gauge K6H019 associated with the different synoptic patterns.

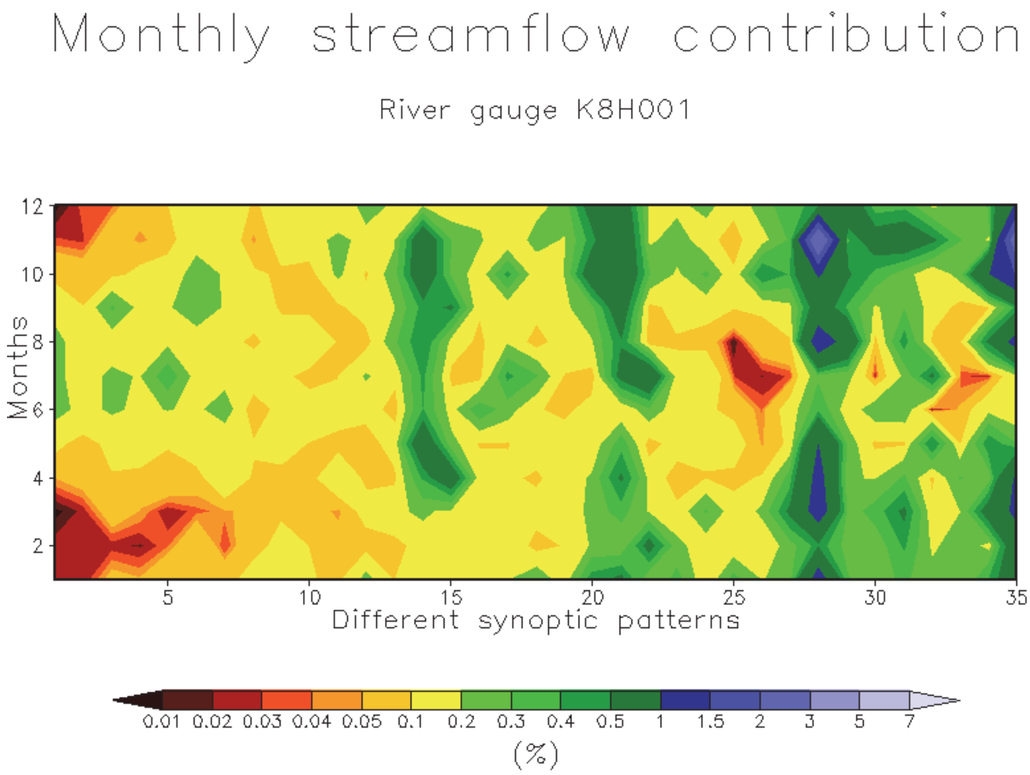

Figure 5.5 Monthly percentage contribution to mean annual streamflow at river gauge K8H001 associated with the different synoptic patterns.

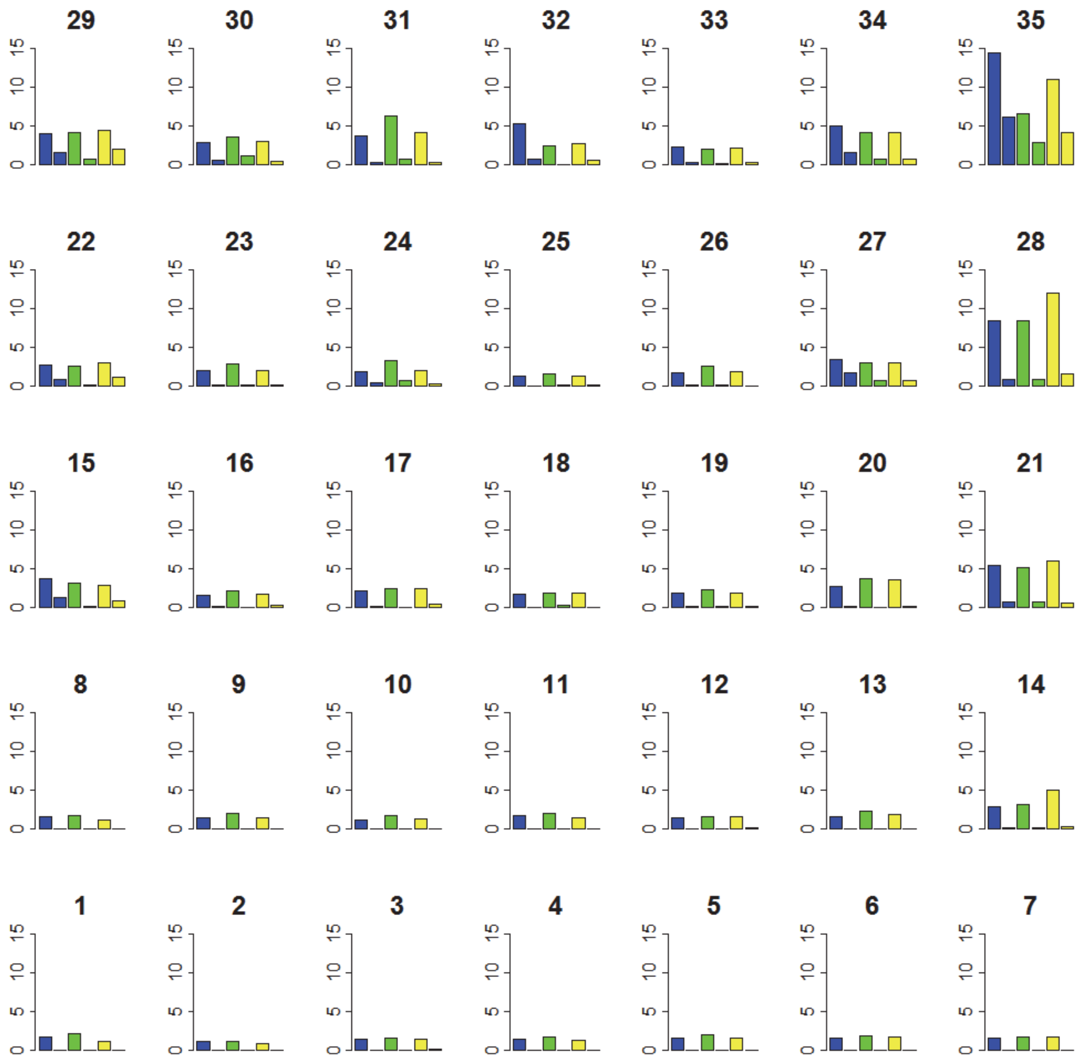

Figure 5.6 Percentage streamflow associated with different weather patterns for river gauges K4H003 (blue), K6H019 (green) and K8H001 (yellow). The right bar for a specific colour is the percentage streamflow associated with COLs.

5.4 Summary

Streamflow in the Cape south coast region is fairly evenly distributed over the year, consistent with the region experiencing all-year rainfall, except over the eastern parts where clear peaks can be discerned for the winter and spring months. The August peak observed in several stations over the eastern parts is particularly striking.

Ridging high-pressure systems are associated with the most notable daily streamflow values observed over the western parts of the study area. Other circulation patterns associated with notable streamflow contributions are circulation patterns 14 (ridge from the southwest), 15 (tropical-temperate trough), 20 (ridge from the southwest), 21 (ridge from the southwest), 27 (ridge from the southwest), 28 (ridge from the southwest), 29 (ridge from the southeast), 30 (ridge from the southeast), 31 (ridge from the southeast), 32 (tropical-temperate trough), 33 (tropical-temperate trough) and 34 (tropical-temperate trough). The single synoptic type associated with the largest contribution to mean annual streamflow at the measuring points considered is the strong ridging high-pressure system. Half of this contribution is associated with COLs.

Chapter 6: Conclusions and Recommendations

The Cape south coast of South Africa, here defined as the region between 21 ˚E and 27 °E and south of the Cape Folded mountains (that is, south of about 33.7 °S), is an all-year rainfall region. Over this region, at least 11 but mostly all 12 months of the year contribute 5 % or more to the long-term average annual rainfall total, in both gridded (CRU TS3.1 and FEWS) and weather station data analysed over the region. Other features that distinguish the region from the winter and summer rainfall regions of South Africa is the relatively high ratio of the rainfall total for the month of minimum rainfall to the total for the month of maximum rainfall, and the relatively small average fluctuation of monthly rainfall totals around the monthly mean rainfall total.

The SOM technique was used to develop a synoptic climatology for the Cape south coast of South Africa, and the synoptic forcing of rainfall over the region was subsequently analysed. Here NCEP reanalysis daily SLP anomaly data were used to train a 7x5 SOM. SLP was selected as the metric for synoptic typing due to the Cape south coast region being close to sea-level. A number of well-known synoptic classes, such as ridging highs, tropical-temperate troughs and weak synoptic flow have been identified by the SOM, as well as subtle but systematic differences within different synoptic types that make up the main classes. The importance of the SOM to capture these subtle differences is illustrated by the nodes' very different contributions to annual rainfall over the region. This is applicable in particular to the rain-producing synoptic types, such as ridging high pressure systems from the southwest and tropical-temperate troughs. For example, the results presented in this report indicate that ridging high pressure systems where the ridge is located further southwards are more conducive to rainfall along the Cape south coast region than ridges located more equatorwards, even if the pressure distribution is otherwise similar. A similar observation was made regarding the intensity of the ridging high pressure systems. It has long been known that the geographical location and the intensity of ridging high pressure systems is a determining factor for the occurrence of rainfall and the nature of the rainfall over the Cape south coast region (e.g. Taljaard, 1996). However, by application of a SOM, it is possible to quantify the rainfall associated with the different types within a main synoptic class. For example, over the 33-year period node 27 (ridging high pressure system from the southwest) yielded 3.6 mm/day, whereas node 28 (also a ridging high- pressure system from the southwest) yielded 5.8 mm/day. Similarly, ridging high pressure systems from the southwest represented by nodes 20 and 21 yielded approximately 1.6 and 3.6 mm/day. Taking the frequency of occurrence of the synoptic types into account, the contribution by a single type within a main synoptic class (e.g. ridging highs) becomes important with regard to seasonal or annual rainfall totals.

Ridging high pressure systems are the synoptic types that contribute most to rainfall totals over the Cape south coast region. These systems have a frequency of occurrence of 23% (of the total number of daily occurrences of synoptic types) but contribute 46% of the total rainfall over the Cape south coast. Tropical-temperate troughs are responsible for 28% of the rainfall. The frequency of occurrence of the various configurations of tropical-temperate troughs accumulates to 25%. COLs occur in combination with ridging high pressure systems (ridging from the southwest and southeast) and tropical-temperate troughs. However, the contribution to rainfall by COLs has been isolated from these systems for comparison purposes using an objective tracking algorithm. COLs contribute 16% (7% in co-occurrence with ridging highs) to the annual rainfall. The contribution to rainfall by COLs is remarkable, considering that the COL-induced rainfall days over the Cape south coast region amount only to 4.2%. Transient frontal troughs were found to bring the least rain of the rain-bearing systems, consistent with the observations of the winter months being associated with a season characterized by lower rainfall totals compared to transitional seasons. The estimated relative contribution of synoptic types to annual rainfall depends to some extent on the spatial coverage and distribution of the weather stations recording rainfall.

The autumn and August rainfall peaks observed in the annual rainfall cycle over the Cape south coast cannot be attributed to a single rain-producing synoptic type. Both ridging highs, tropical-temperate troughs and COLs have been shown to contribute to these rainfall peaks, but with COLs driving the rainfall peak during April. The September hiatus in rainfall that occurs after the August peak, seems to be related to a poleward displacement of frontal systems and positioning of high pressure systems (ridging mainly over land) that are both unfavorable for rainfall. Along the Cape south coast, the October rainfall peak is the highest rainfall peak observed during the year. This rainfall peak is the result of ridging high pressure systems and to a lesser extent tropical-temperate troughs, with an insignificant contribution by COLs. Noteworthy is the importance of ridging high pressure systems relative to COLs for the existence of the October rainfall peak along the coast.

The association between interannual variability of seasonal rainfall over the Cape south coast of South Africa and synoptic types was also investigated. The method of SOMs was employed to relate daily low-level circulation fields obtained from NCEP with daily area-averaged rainfall for the period 1979 to 2011. The daily circulation statistics obtained from the SOM analysis were employed to determine seasonal anomaly fields for each SOM node for seasons of above-normal, near-normal and below-normal rainfall totals. Similarly, rainfall anomalies relative to the climatological mean as well as the average percentage of rainfall associated with each node for seasons of above-normal, near-normal and below-normal rainfall were determined. Analysis of synoptic type frequencies illustrated that, based on the frequency anomaly relative to the climatological frequency of the synoptic types, it is possible to distinguish anomalously wet DJF, MAM and JJA seasons from being anomalously dry. During SON, a discernable difference in the frequency of synoptic types is absent. During wet seasons, the main rainfall-producing synoptic types, representative of ridging high pressure systems and tropical-temperate troughs, occur more frequently. Noteworthy is that these synoptic types remain the main rain-producing synoptic types during dry seasons, but with an anomalously low frequency of occurrence. Being able to use synoptic type frequencies to discriminate between wet and dry seasons has potential implications for seasonal forecasting over the Cape south coast with regard to the confidence in discriminating between an above-normal or below-normal rainfall outlook. Skillful predictions of the differential synoptic type distributions for wet and dry seasons may be a requirement of skillful intra-rainfall prediction over the region.

Rainfall-producing westerly waves nearing the subcontinent are weakly linked to interannual variability of JJA rainfall, even though these systems are not regarded as the main rainfall-producing synoptic types over the Cape south coast. Indeed, during MAM and SON some configurations of westerly wave associated rain are negatively correlated with the respective seasonal rainfall totals. Rainfall associated with the main synoptic types representative of ridging high pressure systems and tropical-temperate troughs are linked to interannual variability of seasonal rainfall. A strong link is suggested for high pressure systems ridging from the southwest during DJF, MAM, JJA and SON while ridges east/southeast of the subcontinent and tropical-temperate troughs exhibit seasonality in it's link to interannual variability of seasonal rainfall over the Cape south coast. Ridges east/southeast of the subcontinent exhibit a stronger link during DJF and MAM compared to JJA and SON while a link between tropical-temperate troughs is indicated to exist only during DJF and MAM. Specific configurations of ridging high pressure systems that are linked to interannual variability of seasonal rainfall, exhibit their ridging axis to be located further polewards (in particular nodes 28 and 35) than those not directly linked to interannual variability of seasonal rainfall. Both these nodes (28 and 35) are representative of weather systems with strong upper-air control. Node 35 is associated with the occurrence of COLs, while node 28 is associated with sharp upper-air troughs. The specific tropical-temperate trough configuration linked to interannual variability of DJF rainfall is suggestive of a slower moving tropical-temperate trough (node 32) with the zonal wind exhibiting similar characteristics to those of wet summers over the summer rainfall region of South Africa (Tennant and Reason, 2005). The zonal wind characteristics associated with node 32 are in contrast to the mean circulation associated with wet winters over the winter rainfall region when an anomalously strong jet is found just upstream of the subcontinent (Reason and Rouault, 2005) that has also been linked to El Niño conditions (Philippon et al., 2012). In general, this node (node 32) occurs mostly in La Niña years. The DJF seasons corresponding with the 10 DJF seasons of the highest occurrence of this node (node 32), display a preference for La Niña years as it consists of 5 La Niña years, 2 El Niño years and 3 neutral years.

A strong link is suggested between COL-induced rainfall and rainfall variability over the Cape south coast for MAM, JJA and SON, with the strongest link found for JJA. Winter is also the season when the mean contribution by COLs to seasonal rainfall totals is the largest in the region (Favre et al., 2013; Engelbrecht et al., 2015). Regarding the geographical location of COLs, there seem to be distinct regions of preferred occurrence during wet and dry seasons, with anomalously more COLs located over the country during wet seasons, in particular over the southern and western parts. Finally, the association between synoptic circulation and streamflow has been quantified and shows the importance of COLs with regard to streamflow contribution and hence water reservoir levels.

In summary:

- The all-year rainfall region is characterized by a relatively small average fluctuation of monthly rainfall totals around the monthly mean rainfall total.
- Synoptic classes, such as ridging highs, tropical-temperate troughs and westerly troughs have been objectively identified by application of the SOM technique on NCEP reanalysis daily SLP anomaly data over a 33-year period.
- Ridging high pressure systems are associated with the largest contribution to rainfall over the all-year rainfall region (46%), followed by tropical-temperate troughs (28%) and COLs (16% of which 7% is in co-occurrence with ridging highs).
- The SOM technique made it possible to isolate certain configurations of a particular synoptic type with regard to its relative rainfall contribution. For example, ridging high pressure systems where the ridge is located further to the south are more conducive to rainfall along the Cape south coast than ridges located more equatorwards.
- The autumn and August rainfall peaks over the Cape south coast are caused by ridging highs, tropical-temperate troughs and COLs but with COLs driving the April rainfall peak.
- The October rainfall peak is driven by ridging highs and to a lesser extent tropical-temperate troughs with an insignificant contribution by COLs.
- Based on synoptic type frequencies, it is possible to distinguish anomalously wet DJF, MAM and JJA seasons from being anomalously dry.
- During wet seasons, rainfall producing synoptic systems such as ridging highs and tropical-temperate troughs occur more frequently.
- Ridging highs, tropical-temperate troughs and COLs are linked to interannual variability of seasonal rainfall.
- The preferred geographical location of COLs during wet and dry seasons differ, with anomalously more COLs located over the country during wet seasons.
- The association between synoptic circulation and streamflow has been quantified. The importance of COLs to streamflow has been illustrated.

Further work is required to determine whether the seasonal frequencies of synoptic types associated with anomalous rainfall over the Cape south coast are related to global modes of variability such as ENSO and SAM. Further research is also needed to determine whether the intraseasonal variability of synoptic types over the Cape south coast region is predictable at the seasonal timescale. To inform decision making at multi-decadal timescales (climate change timescales) it is important to determine how regional climate change will manifest in the changing frequencies of occurrence and intensities of those synoptic types that are important in terms of anomalously dry and wet seasons over the Cape south coast regions.

References

Barclay JJ, Jury MR, Landman W (1993) Climatological and Structural Differences Between Wet and Dry Troughs over Southern Africa in the Early Summer. Meteorology and Amospheric Physics 51: 41-54

Barnston AG, Tippett MK, L'Heureux ML, Li S, DeWitt DG (2011) Skill of real-time seasonal ENSO model predictions during 2002-2011: Is our capability increasing? Bulletin of the American Meteorology Society 93:631-651.doi:10.1175/BAMS-D-11-00111.1

Christensen J.H and Co-authors. (2007) Regional climate projections. Climate Change 2007: The Physical Science Basis, S. Solomon et al, Eds., Cambridge University Press, 849-940.

Cook C, Reason CJC, Hewitson BC (2004) Wet and dry spells within particular wet and dry summers in the South African summer rainfall region. Climate Research 26: 17-31

Crétat J, Richard Y, Pohl B, Rouault M, Reason C, Fauchereau N (2012) Recurrent daily rainfall patterns over South Africa and associated dynamics during the core of the austral summer. International Journal of Climatology 32:261-273. doi:10.1002/joc.2266

Crimp SJ, van den Heever SC, D'Abreton PC, Tyson PD, Mason SJ (1997) Mesoscale modelling of tropical-temperate troughs and associated systems over southern Africa. WRC Report 595/1/97, 395 pp

Engelbrecht CJ, Landman WA (2015). Interannual variability of seasonal rainfall over the Cape south coast of South Africa and synoptic type association. Climate Dynamics DOI: 10.1007/s00382-015-2836-2

Engelbrecht CJ, Landman WA, Engelbrecht FA, Malherbe J (2015) A synoptic decomposition of rainfall over the Cape south coast of South Africa. Climate Dynamics 44: 2589-2607. DOI: 10.1007/s00382-014-2230-5

Engelbrecht CJ, Engelbrecht FA, Dyson LL (2013) High-resolution model-projected changes in mid-tropospheric closed-lows and extreme rainfall events over southern Africa. International Journal of Climatology 33: 173-187. DOI: 10.1002/joc.3420

Fauchereau N, Pohl B, Reason CJC, Rouault M, Richard Y (2009) Recurrent daily OLR patterns in the Southern Africa/Southwest Indian Ocean region, implications for South African rainfall and teleconnections. Climate Dynamics 32: 575-591. DOI: 10.1007/s00382-008-0426-2

Favre A, Hewitson B, Tadross M, Lennard C, Cerezo-Mota R (2012) Relationships between Cut-off Lows and the Semiannual and Southern Oscillations. Climate Dynamics 38: 1473-1487. DOI: 10.1007/s00382-011-1030-4

Favre A, Hewitson B, Lennard C, Cerezo-Mota R, Tadross M (2013) Cut-off lows in the South Africa region and their contribution to precipitation. Climate Dynamics 41: 2331-2351. DOI: 10.1007/s00382-012-1579-6

Fogt RL, Bromwich DH, Hines KM (2011) Understanding the SAM influence on the South Pacific ENSO teleconnection. Climate Dynamics 36: 1555-1576

Gong T, Feldstein SB, Luo D (2010) The impact of ENSO on wave breaking and southern annular mode events. Journal of Atmospheric Science 67: 2854-2870

Harris I, Jones, PD, Osborn TJ, Lister DH (2014) Updated high-resolution grids of monthly climatic observations – the CRU TS3.10 dataset. International Journal of Climatology 34: 623-642. DOI: 10.1002/joc.3711

Harrison MSJ (1984) A generalized classification of South African rain-bearing synoptic systems. International Journal of Climatology 4: 547-560

Hart NCG, Reason CJC, Fauchereau N (2010) Tropical-Extratropical Interactions over Southern Africa: Three Cases of Heavy Summer Season Rainfall. Monthly Weather Review 138: 2608-2623

Hart NCG, Reason CJC, Fauchereau N (2012) Building a Tropical-Extratropical Cloud Band Metbot. Monthly Weather Review 140: 4005-4016

Hart NCG, Reason CJC, Fauchereau N (2013) Cloud bands over southern Africa: seasonality, contribution to rainfall variability and modulation by the MJO. Climate Dynamics 42: 1199-1212. DOI: 10.1007/s00382-012-1589-4

Holloway A, Fortune G, Zweig P, Barrett L, Benjamin A, Chasi V, de Waal J (2012) Eden and Central Karoo Drought Disaster 2009-2011; "The Scramble for Water." For the Provincial Disaster Management Centre, Western Cape by the Disaster Mitigation for Sustainable Livelihoods Programme, Department of Geography and Environmental Studies, Stellenbosch University. 158 pp.

Jury MR, Pathack BMR, Sohn BJ (1992) Spatial structure and interannual variability of summer convection over southern Africa and the SW Indian Ocean. South African Journal of Science 88: 275-280

Jury MR, Levey K (1993) The climatology and characteristics of drought in the eastern Cape of South Africa. International Journal of Climatology 13: 629-641

Hayward LQ, van den Berg H (1968) Die Port Elizabeth-stortreens van 1 September 1968. SA Weather Bureau News Letter No. 234, 157-169

Hayward LQ, van den Berg H (1970) The Eastern Cape Floods of 24 to 28 August, 1970. SA Weather Bureau News Letter No. 257, 129-141

Hewitson BC, Crane RG (2002) Self-organizing maps: Applications to synoptic climatology. Climate Research 22: 13-26

Jury MR, Levey K (1993) The climatology and characteristics of drought in the eastern Cape of South Africa. International Journal of Climatology 13: 629-641. DOI: 10.1002/joc.3370130604

Kalnay E, Kanamitsu M, Kistler R, Collins W, Deaven D, Gandin L, Iredell M, Saha S, White G, Woollen J, Zhu Y, Leetmaa A, Reynolds B, Chelliah M, Ebisuzaki W, Higgins W, Janowiak J, Mo KC, Ropelewski C, Wang J, Jenne R, Joseph D (1996) The NCEP/NCAR 40-year reanalysis project. Bulletin of the American Meteorological Society 77: 437-471

Katzfey JJ, McInnes KL (1996) GCM simulations of Eastern Australia cut-off lows. Journal of Climate 9: 2337-2355

Kohonen T (2001) Self-Organizing Maps. 3rd ed. Springer, 501 pp

Landman WA, Mason SJ, Tyson PD, Tennant WJ (2001) Retro-active skill of multi-tiered forecasts of summer rainfall over southern Africa. International Journal of Climatology 21: 1-19

Landman WA, Mason SJ, Tyson PD and Tennant WJ (2001) Statistical downscaling of GCM simulations to Streamflow. Journal of Hydrology 252: 221-236

Landman WA, Kgatuke MJ, Mbedzi M, Beraki A, Bartman A and du Piesanie A (2009) Performance comparison of some dynamical and empirical downscaling methods for South Africa from a seasonal climate modeling perspective. International Journal of Climatology 29: 1535-1549 DOI:10.1002/joc.1766

Landman WA, Beraki A (2012) Multi-model forecast skill for mid-summer rainfall over southern Africa. International Journal of Climatology 32: 303-314. DOI:10.1002/joc.2273

Landman WA, DeWitt D, Lee DE, Beraki A, Lötter D (2012) Seasonal Rainfall Prediction Skill over South Africa: One- versus Two-Tiered Forecasting Systems. Weather and Forecasting 27:489-501

Lennard C, Hegerl G (2015) Relating changes in synoptic circulation to the surface rainfall response using self-organizing maps. Climate Dynamics 44: 861-879 DOI:10.1007/s00382-014-2169-6

L'Heureux ML, Thompson DWJ (2006) Observed relationships between the El Niño-Southern Oscillation and the extratropical zonal-mean circulation. Journal of Climate 19: 276-287

Malherbe J, Engelbrecht FA, Landman WA, Engelbrecht CJ (2012) Tropical systems from the southwest Indian Ocean making landfall over the Limpopo River Basin, southern Africa: a historical perspective. International Journal of Climatology 32: 1018-1032. DOI: 10.1002/joc.2320

Malherbe J, Landman WA, Olivier C, Sakuma H, Luo J- J (2014) Seasonal forecasts of the SINTEX-F coupled model applied to maize yield and streamflow estimates over north-eastern South Africa. Meteorological Applications 21: 733-742. doi:10.1002/met.1402

Malherbe J, Landman WA, Engelbrecht FA (2014a) The bi-decadal rainfall cycle, Southern Annular Mode and tropical cyclones over the Limpopo River Basin, southern Africa. Climate Dynamics 42:3121-3138. DOI 10.1007/s00382-013-2027-y

Mason SJ, Jury MR (1997) Climatic variability and change over southern Africa: a reflection on underlying processes. Progress in Physical Geography 21: 23-50

Mo KC (2000) Relationships between Low-Frequency Variability in the Southern Hemisphere and Sea Surface Temperature Anomalies. Journal of Climate 13: 3599-3610

Muller A, Reason CJC, Fauchereau N (2008) Extreme rainfall in the Namib Desert during summer 2006 and influences of regional ocean variability. International Journal of Climatology 28: 1061-1070. doi:10.1002/joc.1603

Nel J, Le Maitre D, Smith J (2013) An introduction to South Africa's water source areas. Council for Scientific and Industrial Research, Report

Philippon N, Rouault M, Richard Y, Favre A (2011) The influence of ENSO on winter rainfall in South Africa. International Journal of Climatology 32: 2333-2347. DOI: 10.1002/joc.3403

Pohl B, Fauchereau N, Reason CJC, Rouault M (2010) Relationships between the Antarctic Oscillation, the Madden-Julian Oscillation, and ENSO, and consequences for rainfall analysis. Journal of Climate 23: 238-254

Pohl B, Rouault M, Sen Roy S (2014) Similation of the annual and diurnal cycles of rainfall over South Africa by a regional climate model. Climate Dynamics 43: 2207-2226. DOI: 10.1007/s00382-013-2046-8

Reason CJC, Allan RJ, Lindesay JA, Ansell TJ (2000) ENSO and climatic signals across the Indian Ocean basin in the global context: Part I, interannual composite patterns. International Journal of Climatology 20: 1285-1327

Reason CJC, Rouault M, Melice JL, Jagadheesha D (2002) Interannual winter rainfall variability in SW South Africa and large scale ocean-atmosphere interactions. Meteorology and Atmospheric Physics 80: 19-29

Reason CJC, Rouault M (2005) Links between the Antarctic Oscillation and winter rainfall over western South Africa. Geophysical Research Letters 32: L07705. 10.1029/2005GL022419

Roberts CPR, Alexander WJR (1982) Lessons learnt from the 1981 Laingsburg flood. Civil Engineer in South Africa 24: 17-21, 24-25, 27

Rouault M, White SA, Reason CJC, Lutjehams JRE, Jobard I (2002) Ocean-Atmosphere interaction in the Agulhas current region and a South African extreme Weather event. Weather and Forecasting 17: 655-669

Rouault M, Richard Y (2003) Intensity and spatial extension of drought in South Africa at different time scales. Water SA 29: 489-500

Schuenemann KC, Cassano JJ, Finnis J (2009) Synoptic forcing of precipitation over Greenland: climatology for 1961-99. Journal of Hydrometeorology 10: 60-78

Singleton AT, Reason CJ (2006) Numerical simulations of a severe rainfall event over the Eastern Cape coast of South Africa: sensitivity to sea surface temperature and topography. Tellus 58: 355-367

Singleton AT, Reason CJ (2007a) A numerical model study of an intense cutoff low pressure system over South Africa. Monthly Weather Review 135: 1128-1150

Singleton AT, Reason CJ (2007b) Variability in the characteristics of cut-off low pressure systems over subtropical southern Africa. International Journal of Climatology 27: 295-310

Smith TM, Reynolds RW, Peterson TC, Lawrimore J (2008) Improvements to NOAA's Historical Merged Land-Ocean Surface Temperature Analysis (1880-2006). Journal of Climate 21:2283-2296

Sylla MB, Giorgi F, Coppola E, Mariotti L (2013) Uncertainties in daily rainfall over Africa: assessment of gridded observation products and evaluation of a regional climate model simulation. International Journal of Climatology 33: 1805-1817. DOI: 10.1002/joc.3551

Taljaard JJ (1985) Cut-off lows in the South African region. South African Weather Bureau, Technical paper 14

Taljaard JJ (1995) Atmospheric circulation systems, synoptic climatology and weather phenomena of South Africa. Part 2: Atmospheric circulation systems in the South African region. South African Weather Bureau, Technical paper 28

Taljaard JJ (1996) Atmospheric circulation systems, synoptic climatology and weather phenomena of South Africa. Part 6: Rainfall in South Africa. South African Weather Bureau, Technical paper 32

Tennant WJ, van Heerden J (1994) The influence of orography and local sea-surface temperature anomalies on the development of the 1987 Natal floods: a general circulation model study. Suid-Afrikaanse Tydskrif vir Wetenskap 90: 45-49

Tennant WJ, Hewitson BC (2002) Intra-seasonal rainfall characteristics and their importance to the seasonal prediction problem. International Journal of Climatology 22: 1033-1048. DOI: 10.1002/joc.778

Tennant WJ (2003) An assessment of intraseasonal variability from 13-yr GCM Simulations. Monthly Weather Review 131: 1975-1991

Tennant WJ (2004) Considerations when using pre-1979 NCEP/NCAR reanalysis in the southern hemisphere. Geophysical Research Letters 31: L11112. DOI: 10/1029/2004GLO197501

Tennant WJ, Reason CJC (2005) Associations between the Global Energy Cycle and Regional Rainfall in South Africa and Southwest Australia. Journal of Climate 18: 3032-3047

Todd M, Washington R, Palmer PI (2004) Water vapour transport associated with tropical-temperate trough systems over southern Africa and the southwest Indian Ocean. International Journal of Climatology 24: 555-568

Tozuka T, Abiodun BJ, Engelbrecht FA (2014) Impacts of convection schemes on simulating tropical-temperate troughs over southern Africa. Climate Dynamics 42: 433-451

Van Heerden J, Terblance DE, Schulze GC (1988) The Southern Oscillation and South African summer rainfall. Journal of Climate 8: 577-597

Van Rooy MP (1972) Climate of South Africa: District rainfall for South Africa and the annual march of rainfall over southern Africa, part 10. South African Weather Bureau Tech. Note WB 35, Dept. of Transport, Pretoria, South Africa, 116 pp.

Van Schalkwyk L, Dyson LL (2013) Climatological characteristics of fog at Cape Town International airport. Weather and Forecasting 28: 631-646. DOI: 10.1175/WAF-D-12-00028.1

Washington R, Todd M (1999) Tropcial-temperate links in the Southern African and southwest Indian Ocean satellite-derived daily rainfall. International Journal of Climatology 19: 1601-1616

Washington R, Preston A (2006) Extreme wet years over southern Africa: Role of Indian Ocean sea surface temperatures. Journal of Geophysical Research 111: D15104, DOI:10.1029/2005JD006724

Weepener HL, van den Berg HM, Metz M, Hamandawana H (2012) The development of a hydrologically improved Digital Elevation Model and derived products for South Africa based on the SRTM DEM. Water Research Commission, Pretoria. Report No. 1908/1/11. Press ISBN 978-1-4312-0217-1

Weldon D, Reason CJC (2014) Variability of rainfall characteristics over the South Coast region of South Africa. Theoretical and Applied Climatology 115: 177-185. DOI: 10.1007/s00704-013-0882-4

Wilks DS (2011) Statistical methods in the atmospheric sciences, 3rd edn. Academic Press, Amsterdam